LBL-10546
Preprint

Lawrence Berkeley Laboratory
UNIVERSITY OF CALIFORNIA

EARTH SCIENCES DIVISION

Submitted for publication to Water Resources Research

CHEMICAL TRANSPORT IN A FISSURED ROCK: VERIFICATION OF A NUMERICAL MODEL

A. Rasmuson, T.N. Narasimhan, and I. Neretnieks

April 1982

Prepared for the U.S. Department of Energy under Contract DE-AC03-76SF00098

DISCLAIMER

LBL-10546

CHEMICAL TRANSPORT IN A FISSURED ROCK:

VERIFICATION OF A NUMERICAL MODEL

A. Rasmuson[1], T. N. Narasimhan[2], and I. Neretnieks[1]

1 Department of Chemical Engineering
Royal Institute of Technology
S-100 44 Stockholm, Sweden

2 Earth Sciences Division
Lawrence Berkeley Laboratory
University of California
Berkeley, California 94720

This work was supported by the Director, Office of Energy Research, Office of Basic Energy Sciences, Division of Engineering, Mathematics, and Geosciences of the U. S. Department of Energy under Contract DE-AC03-76SF00098. Funding for Rasmuson and Neretnieks was provided by the Nuclear Fuel Safety Project, Sweden.

TABLE OF CONTENTS

LIST OF FIGURES iv

LIST OF TABLES v

ABSTRACT 1

INTRODUCTION 2

THEORY 9
Differential Formulation 9
Chemical Transport in the Fracture 9
Chemical Transport in the Rock. 11
Depth of Nuclide Penetration 14
Integral Formulation 17
Numerical Scheme 19
Estimating Interface Concentration to Compute Advective Solute Transfer. 22
Estimating Interface Gradient to Compute Conductive Solute Transfer 24
The Discretized Equations 24

RESULTS 28
Problem 1: One-dimensional Transport in a Single Fracture . . 30
Problem 2: Advective-Dispersion in Parallel Fractures with Diffusion in Rock Matrix: Early Time Solution (Nonpenetrating Case) 34
Problem 3 Advection-Dispersion in a Set of Parallel Fractures with Diffusion in Microfissured Matrix: Large-time Solution (Penetrating Case) 43
Problem 4: Case 2 with Radioactive Decay. 47
Problem 5: Case 3 with Radioactive Decay. 50

SENSITIVITY ANALYSIS 50

CONCLUSIONS 54

ACKNOWLEDGMENTS 54

REFERENCES. 54

NOTATION 58

LIST OF FIGURES

Figure 1. Sketch of concentration break-through at a point in a one-dimensional advection-diffusion system 5

Figure 2. Influence of input computational errors on concentration break-through 8

Figure 3. Sketch of the fracture-matrix system for the two-dimensional advection-diffusion problem 10

Figure 4. Diffusion in a sphere with constant surface potential c/c_o as a function of R' for various values of T' 16

Figure 5. Definition of volume element, nodal point, interior surface segment, and boundary surface segment for the IFD scheme 18

Figure 6. Schematic IFD mesh with volume element (node) ℓ in the rock matrix communicating into other rock or fracture elements 20

Figure 7. One-dimensional advection-diffusion problem: Effect of upstream weighting at $Pe_\ell = 10.25$ 31

Figure 8. One-dimensional advection-diffusion problem: Effect of Peclet Number at $\zeta = 0.65$ 32

Figure 9. One-dimensional advection-diffusion problem: Comparison of break-through curves with solution for two different Peclet Numbers. 33

Figure 10. Schematic mesh design for advective-diffusion problem, nonpenetration case 38

Figure 11. Nonpenetrating case: Comparison of analytic and numerical solutions for $0.005 < Pe_\ell < 0.041$ and Pe =.19341 41

Figure 12. Nonpenetrating case: Comparison of analytic and numerical solutions for a mesh with $0.5 < Pe_\ell < 4$ and Pe = 19.341 . 42

Figure 13. Penetrating case: Comparison of analytic and numerical solutions for a mesh with $0.0167 < Pe_\ell < 0.111$ and Pe = 0.5 48

Figure 14. Nonpenetrating case with decay: Comparison of analytic and numerical solutions for a mesh with $0.005 < Pe_\ell < 0.041$ and with half-lives of 8×10^5 and 8×10^6 s 49

Figure 15. Penetrating case with decay: Comparison of analytic and numerical solutions for a mesh with $0.0167 < Pe_\ell < 0.111$ and with half-life of 3×10^8 years 51

ABSTRACT

Numerical models for simulating chemical transport in fissured rocks constitute powerful tools for evaluating the acceptability of geological nuclear waste repositories. Due to the very long-term, high toxicity of some nuclear waste products, the models are required to predict, in certain cases, the spatial and temporal distribution of chemical concentration less than 0.001% of the concentration released from the repository. Whether numerical models can provide such accuracies is a major question addressed in the present work. To this end, we have verified a numerical model, TRUMP, which solves the advective diffusion equation in general three dimensions with or without decay and source terms. The method is based on an integrated finite-difference approach. The model was verified against known analytic solution of the one-dimensional advection-diffusion problem as well as the problem of advection-diffusion in a system of parallel fractures separated by spherical particles. The studies show that as long as the magnitude of advectance is equal to or less than that of conductance for the closed surface bounding any volume element in the region (that is, numerical Peclet number <2), the numerical method can indeed match the analytic solution within errors of $\pm 10^{-3}$ % or less. The realistic input parameters used in the sample calculations suggest that such a range of Peclet numbers is indeed likely to characterize deep groundwater systems in granitic and ancient argillaceous systems. Thus TRUMP in its present form does provide a viable tool for use in nuclear waste evaluation studies. A sensitivity analysis based on the analytic solution suggests that the errors in prediction introduced due to uncertainties in input parameters is likely

to be larger than the computational inaccuracies introduced by the numerical model. Currently, a disadvantage in the TRUMP model is that the iterative method of solving the set of simultaneous equations is rather slow when time constants vary widely over the flow region. Although the iterative solution may be very desirable for large three-dimensional problems in order to minimize computer storage, it seems desirable to use a direct solver technique in conjunction with the mixed explicit-implicit approach whenever possible. Work in this direction is in progress.

INTRODUCTION

Since the late 1970's the interest in describing radionuclide migration in subsurface systems has increased considerably. The present interest stems from the need to predict the possible escape of radionuclides from a radioactive waste repository located deep underground. The problem of prediction usually is divided into two parts. The first consists of determining the water movement, and the second, the transport of radionuclides by the water. The water movement in the far field (i.e., far from the repository) is assumed to be independent of the nuclide movement which makes it possible to decouple the two flow fields. The nuclide migration is assumed to be due to both advective transport and diffusion-dispersion and to be influenced by chemical and physical interaction with the solid material. The nuclides decay with time but may also build up in concentration due to decay of a parent.

A well-known mathematical model which includes these effects for one-dimensional flow is the GETOUT model (Lester et al., 1975). This is based on

an analytic solution of the governing equations and includes chain decay. Another model, which has the capability of multidimensional dispersion of the nuclides, has been developed by Dillon et al. (1978). This code is based on a numerical solution of the governing equations using a finite-difference technique. Both these models are based on the concept of an instantaneous, reversible reaction of the nuclide in the water with the solids. Local equilibrium is thus always assumed to be established. Lately it has been questioned (Neretnieks, 1980; Grisak et al. 1980a,b, 1981; Tang et al., 1981) whether this assumption might not be seriously in error for flow in a fissured crystalline rock. This is due to the fact that the water flows in the macrofissures or fractures of the rock which may be fairly widely spaced. The sorption may not take place homogeneously in the rock because the time needed to distribute the nuclides evenly through the rock by diffusion through the stagnant water present in very small microfissures might be too long.

Neretnieks' (1980) analysis of this phenomenon was based on a description of the conditions in a single fissure. Simple analytic solutions could be found for a single nuclide. Rasmuson and Neretnieks (1980, 1981) extended the model to describe the flow in a porous bed consisting of spherical particles and including axial disperion. Rasmuson (1981) also extended the model to include radial dispersion. In these models only one nuclide is considered. Even under such a simple condition, the resulting analytic solutions proved to be quite complicated in their structure and not amenable to straightforward computational evaluation. It was therefore decided in the present study to investigate the capability of a numerical method to handle these systems since

numerical methods appear to offer the only practical way at present to describe more complex situations.

In investigating the numerical method, one of the problems which was given a high priority was to determine the degree of accuracy with which the early part of the nuclide arrival can be simulated. This is of special interest in studying radionuclide migration since a major mechanism for assuring safety is to give the radionuclide sufficient time to decay.

The problem may be illustrated by the following simplified model describing the arrival of a tracer at a point of interest. The concentration c of a tracer which arrives at the observation point at time t after the release at the injection point is described by the function $c_o \cdot f(t)$, where c_o is the inlet concentration. Under certain mathematical linearity conditions the function f is independent of c. This is realistic in many practical cases. The function has the following property for the transport of a single tracer:

$$0 \leqslant f < 1 \qquad (1)$$

A typical breakthrough curve f(t) may look like the one depicted in Figure 1. In many practical applications with stable compounds, the accuracy sought in determining the function f(t) is not very high. In chemical engineering problems for example, better than 0.1% absolute accuracy would normally be deemed adequate. A concentration which is 0.1% of that at the inlet end of an adsorption column, or in a field test with tracers, is often near detection limits and there is usually no need for greater relative accuracy.

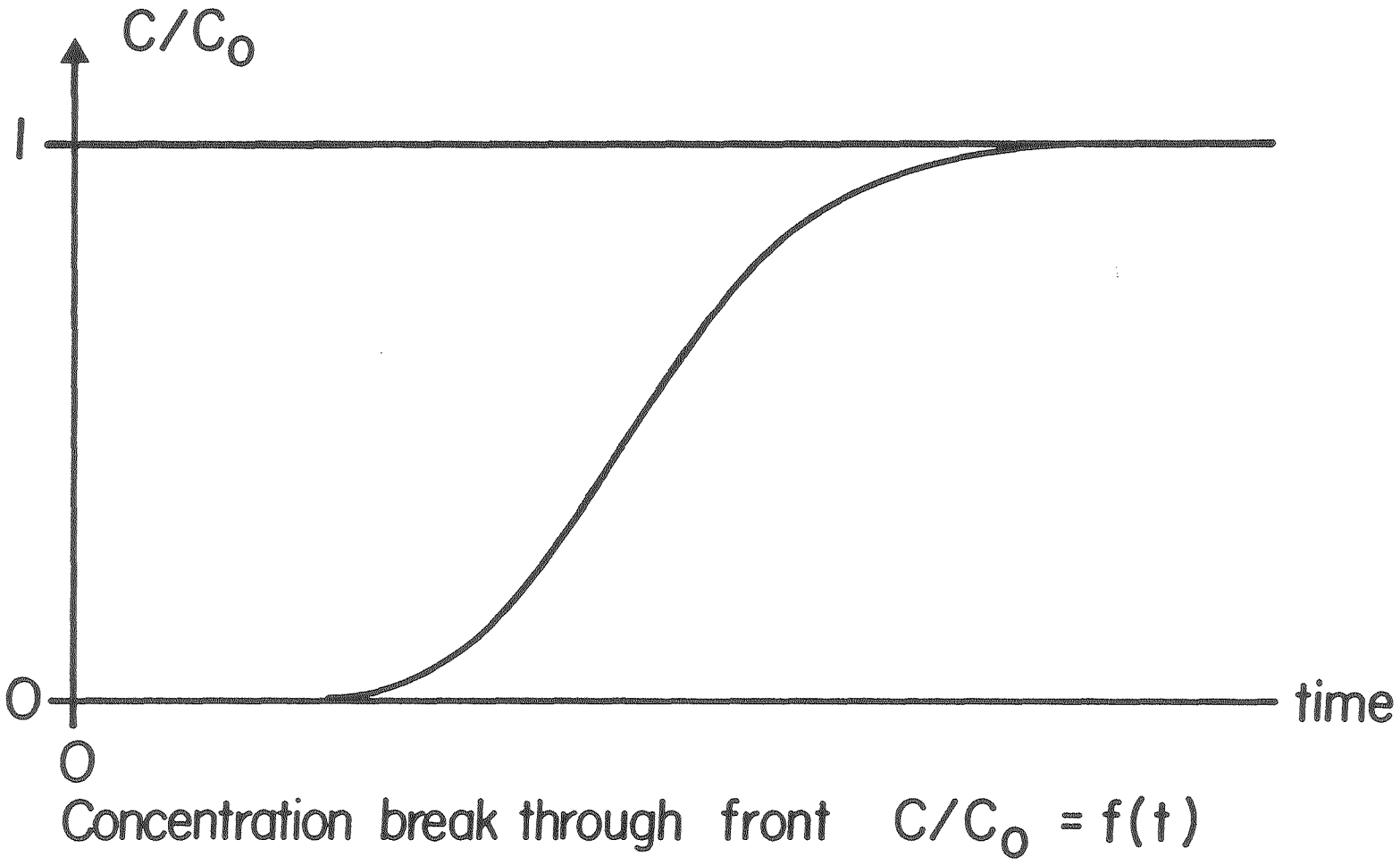

XBL825-2249

Figure 1. Sketch of concentration break-through at a point in a one-dimensional advection-diffusion system. [XBL 825-2249]

The problem is different, however, when large amounts of radioactive materials are handled. Often the radionuclides must not reach the biosphere in concentrations larger than 10^{-9} to 10^{-6} of the concentration at the locus of an accidental leak in a repository. The value 10^{-9} is arrived at in the following way. A thousand-year-old waste has an activity of less than 10^{2} Ci/tonne original fuel (KBS, 1977). The total amount of waste in a repository for the Swedish program--12 reactors running for 30 years--is less than 10,000 tonnes of fuel (KBS, 1978). A maximum leach rate is expected to be 3.3×10^{-5} fractions/year (KBS, 1977). If this amount decreases in activity by 10^{-9} before reaching the biosphere, the inflow to the biosphere is 33×10^{-9} Ci/year. In the KBS safety study (KBS, 1977), which fulfilled the Swedish stipulation law of being safe, at least 11 nuclides were calculated to have many orders of magnitude higher inflow rates. The value 10^{-9} should therefore be a very conservative value. One of the major aims in repository design is to ensure that enough time will be available for a nuclide to decay to safe levels before the nuclide reaches the biosphere.

A concentration of 10^{-6} c_o might be acceptable in certain cases, but not 10^{-5} c_o which is 10 times higher. This means that sometimes there may be a need to predict the early part of the breakthrough curve with a fairly high relative accuracy even though the absolute accuracy is very high.

The relative concentration of a decaying nuclide at a point of interest is the product of the breakthrough curve f(t) and the decay function $\exp[-\lambda_d t]$ where λ_d is the decay constant. We have

$$c/c_o = f(t) \exp [-\lambda_d t] \quad (2)$$

For the linear case mentioned previously, Figure 2 shows that a small absolute error in predicting f(t)--the error is 0.003--may give a ten-fold error in the maximum concentration at the breakthrough point.

The purpose of the present work is to investigate whether relative errors on the order of 0.001% or less are achievable in predictive models of chemical transport using numerical methods. To this end we investigated a widely-used computer program TRUMP (Edwards, 1969) which solves for advective-diffusive heat transport in multidimensional systems. This heat transport code is readily amenable to the chemical transport problem if we recognize the strong similarities between heat and solute transport. Specifically, we applied this program to a system involving fissured massive rock with advection restricted to fissures and diffusion through stagnant pore fluid being the only transport mechanism active in the microfissured rock mass. Our goal was to validate the numerical model through comparison with known analytic solutions of Neretnieks (1980) and Rasmuson and Neretnieks (1980, 1981). In the present work we will restrict our attention to a steady-state fluid flow field with one chemical species that is subject to decay.

In seeking to formulate the equations governing the problem of interest there is strong reason to believe that considerable advantages could be gained in terms of simplicity and generality if the equations are written directly as integrals. We have attempted to provide a theoretical basis for this reasoning in formulating the governing numerical equations.

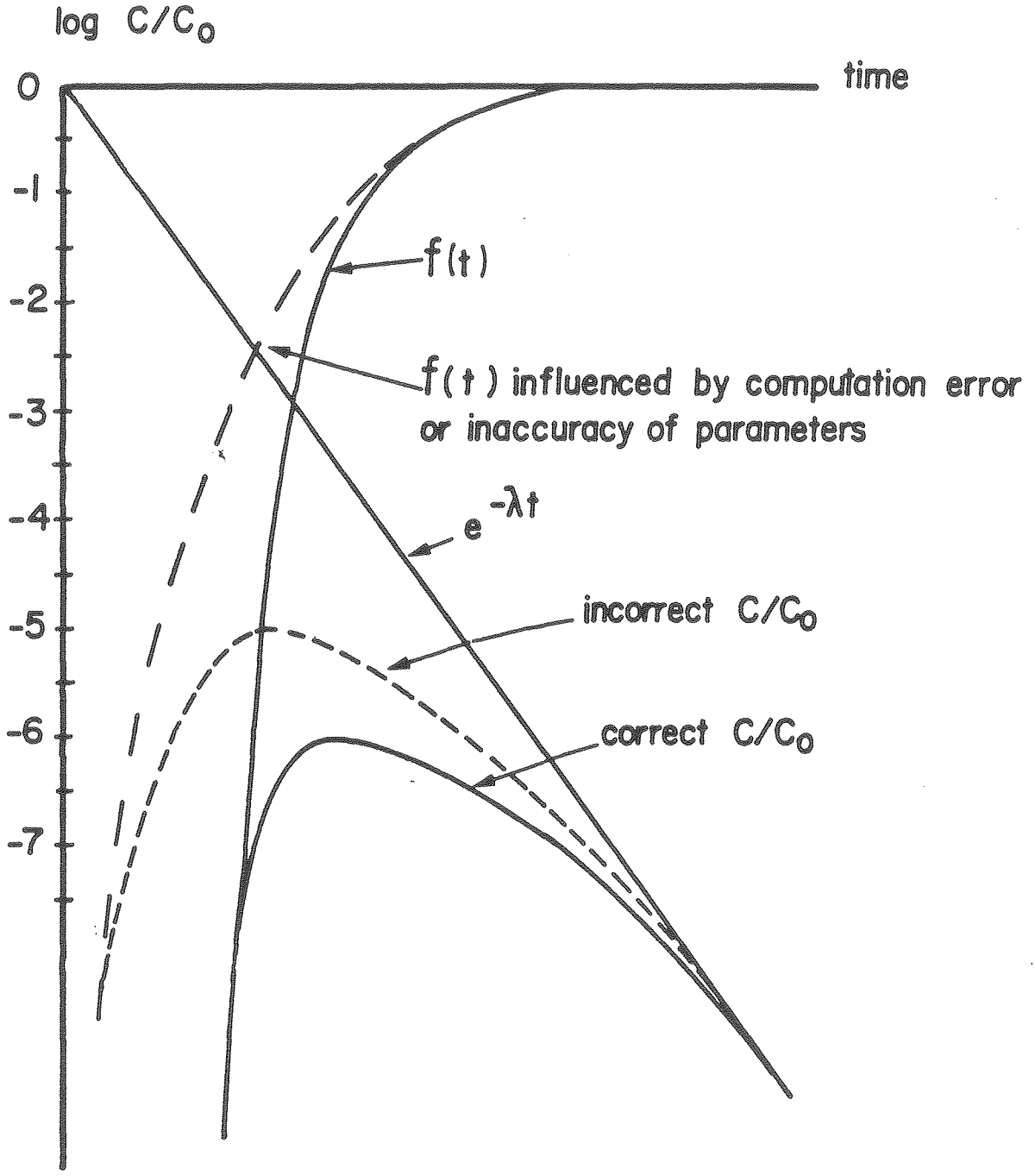

Figure 2. Influence of input computational errors on concentration breakthrough. [XBL 825-2250]

THEORY

In dealing with the chemical transport of nuclides in a fractured rock mass we are concerned with a heterogeneous flow region in which advection is restricted to the fractures while diffusion is dominant in the rock mass. It is customary to describe the physics of this problem through two coupled partial differential equations, one describing advection and longitudinal dispersion in the fractures and the other describing diffusion and sorption in the rock. The coupling is assured through an internal boundary condition demanding continuity of flux and concentration at the fracture-rock interface. Alternately, the same problem could be stated in integral form by writing equations of mass conservation for finite subdomains of the flow region. This representation, which has the advantage of generality for numerical implementation, conveniently dispenses with the need for stating internal boundary conditions. Inasmuch as this report deals with the analytical validation of a numerical method, we shall here present both the formulations.

DIFFERENTIAL FORMULATION

Consider a system of parallel, horizontal fractures separated by unfractured rock as shown in Figure 3. As proposed by Neretnieks (1980) and Rasmuson and Neretnieks (1980) the coupled partial differential equations may be written

Chemical Transport in the Fracture

$$-v_f \frac{\partial c_f}{\partial z} + D_L \frac{\partial^2 c_f}{\partial z^2} - w - \lambda_d c_f = \frac{\partial c_f}{\partial t} \tag{3}$$

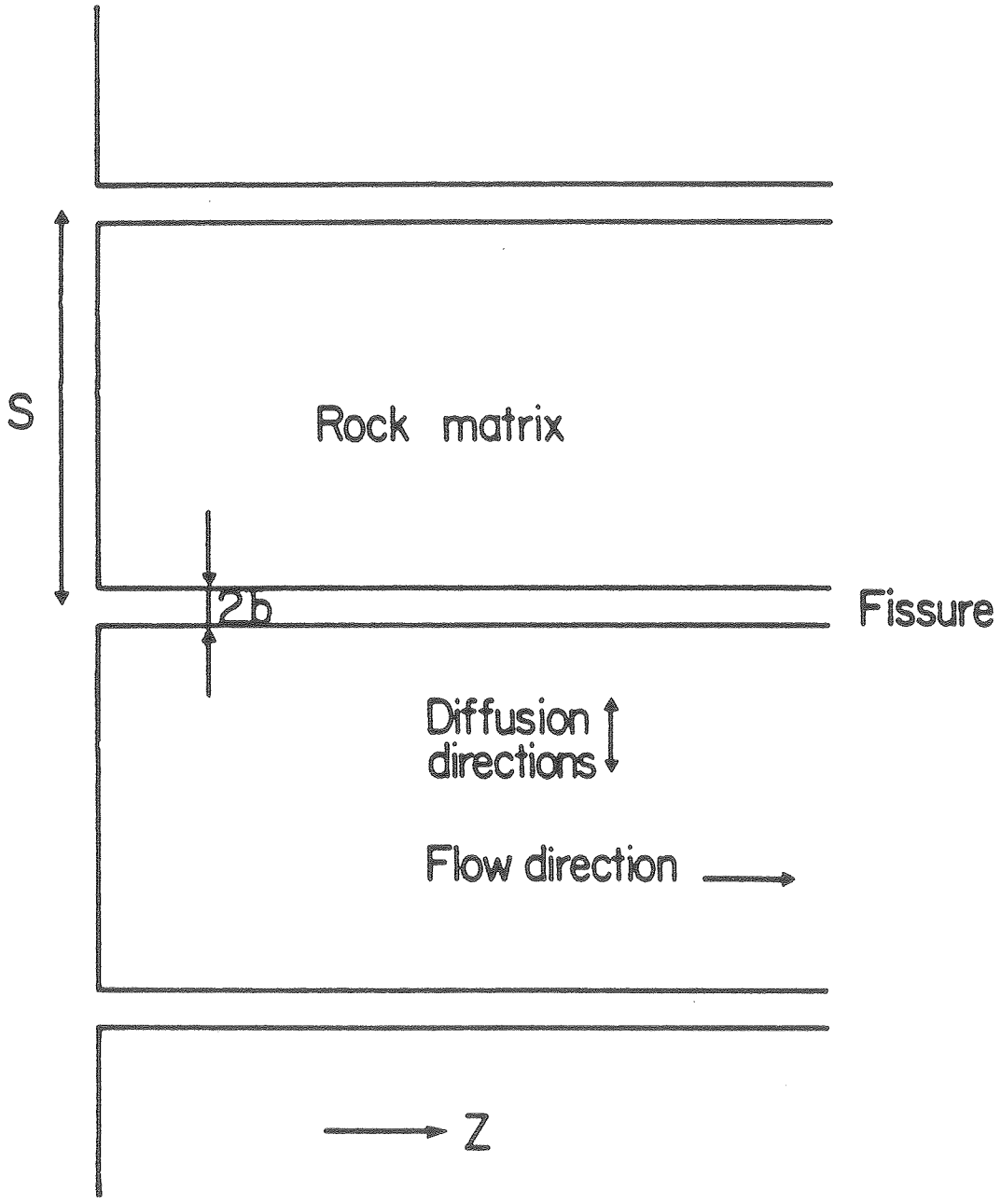

Figure 3. Sketch of the fracture-matrix system for the two-dimensional advection-diffusion problem. [XBL 825-2251]

Chemical Transport in the Rock

$$\nabla \cdot D_p \varepsilon_p \nabla c_p - K\lambda_d c_p = K \frac{\partial c_p}{\partial t} \tag{4}$$

where v_f is the steady-state water velocity in the fracture, c_f is concentration of species in the fracture, D_L is the longitudinal dispersion coefficient for the fracture, z is the coordinate axis oriented along the fracture, w is the coupling term denoting the rate at which the solute is lost from the fracture to the rock matrix per unit volume of the fracture, D_p is the diffusivity of the species in the pore-fluid, ε_p is the porosity of the rock due to the presence of microfissures, λ_d is the decay coefficient, and K is the volume equilibrium constant defined as the mass of solute required to change the pore-fluid concentration, c_p, by unity per unit volume of the rock. The concentration of the species in the solid, c_s and c_p, will not in general be equal. The ratio of c_s to c_p at equilibrium is the partition coefficient K_A, defined by

$$K_A = \frac{c_s}{c_p} \tag{5}$$

In the above, c_s is defined in terms of the bulk volume of the porous matrix. In view of the partition coefficient, K becomes a function of ε_p and K_A. Thus

$$K = \varepsilon_p + K_A. \tag{6}$$

For a nonsorbing species, $K_A = 0$ and

$$K = \varepsilon_p. \tag{7}$$

The rate at which the solute is transferred from the fracture to the adjacent block of rock depends on the diffusivity, the concentration gradient, and the area cross section at the fracture-rock interface. Thus,

$$V_f w = D_{f,r} \left.\frac{\partial c_p}{\partial r}\right|_{f,r} \Gamma_{f,r} \tag{8}$$

where V_f is the fracture volume, $D_{f,r}$ and $\Gamma_{f,r}$ are the diffusivity and area of cross section at the fracture rock block interface. Here, r is the orientation of the transverse axis of diffusion. Note that the quantity of solute lost by fracture is gained by the rock block. Let $\bar{c}_r$ denote the bulk-average concentration of the solute in the rock block comprising the microfissures and the solids. Then,

$$V_f w = V_r \frac{\partial \bar{c}_r}{\partial t} \tag{9}$$

where V_r is the volume of the rock block. If we now define the bulk rock volume V_b to be $V_f + V_r$ and the fracture porosity ε_f by V_f/V_b, then,

$$w = \frac{1 - \varepsilon_f}{\varepsilon_f} \frac{\partial \bar{c}_r}{\partial t} . \tag{10}$$

If the rock matrix associated with the fracture is idealized as spherical (Rasmuson and Neretnieks, 1981), then in equation 4,

$$\nabla \cdot D_p \varepsilon_p \nabla c_p = D_p \varepsilon_p \left[\frac{\partial^2 c_p}{\partial r^2} + \frac{2}{r} \frac{\partial c_p}{\partial r}\right]. \tag{11}$$

The rate of transfer of solute from the fracture to the sphere (equation 8) is

$$V_f w = \left(D_{f,r} \left.\frac{\partial c_p}{\partial r}\right|_{f,r} \right) \left(4\pi r_o^2 \right) \tag{12}$$

where r_o is the radius of the sphere. The average rate of change of concentration in the sphere becomes:

$$\frac{\partial \bar{c}_r}{\partial t} = \frac{V_f w}{V_r} = \frac{3}{r_o} D_{f,r} \left.\frac{\partial c_p}{\partial r}\right|_{f,r} \tag{13}$$

It may be pointed out that since diffusion is assumed to occur only within the rock through the stagnant water present in the microfissures, the interface diffusivity, $D_{f,r}$ in equations (12) and (13) is equal to $D_p \varepsilon_p$.

Essentially, the fractured continuum is treated as a "two-porosity" medium or a complex of two interacting continua. The transfer term represented in equation 13 forms the basis for coupling the two.

The fractured rock system under consideration is subject to the following boundary and initial conditions:

Boundary Conditions:

$$c_f(0, t) = c_o e^{-\lambda_d t} \quad , \qquad \lambda_d \geq 0 \tag{14}$$

$$c_f(\infty, t) = 0 \tag{15}$$

Initial Conditions:

$$c_f(z, 0) = 0 \tag{16}$$

$$c_p(r, z, 0) = 0 \tag{17}$$

We will follow the convention that $r = 0$ at the center of the sphere and $r = r_o$ at the interface between the fracture and the sphere. At the center of the sphere there is a symmetry condition, i.e., $\partial c_p / \partial r = 0$.

Equations (3) and (4), subject to the internal boundary condition (13), the boundary conditions (14) and (15), and the initial conditions (16) and (17), fully characterize the advection-diffusion problem under consideration.

DEPTH OF NUCLIDE PENETRATION

It is pertinent at this juncture to discuss the magnitude of nuclide penetration into the rock matrix as a function of time. The mathematical formulation for the case with no longitudinal dispersion in the fracture and diffusion into rock slabs of infinite extent was given by Neretnieks (1980) together with the analytical solution. This model was subsequently extended by treating the finite block size of the rock as well as longitudinal dispersion in the bedrock (Rasmuson and Neretnieks, 1980,1981). In this model, a cubic system of orthogonal fractures was assumed (Snow, 1968). However, the cubic grid geometry is awkward for modeling internal diffusion. Therefore, the problem was solved by approximating the cubes by spheres having the same surface-to-volume ratio as a cubic block.

The solution of this model may be used to simulate the uptake of finite rock slabs and longitudinal dispersion in the fissures as sketched in Figure 3. It is obvious that at very early times, the advance of the concentration front into the rock matrix is restricted to a very thin layer, close to the fracture-rock interface. This short penetration-depth allows the approximation of the flat wall by a thin spherical shell.

Further, the slab is approximated by spheres having the same surface-to-volume ratio as a slab. This implies that the total surface area contacted by

the water is the same for the sphere as it would be for the slab and the amount of solid in the bed is the same. This approximation gives exactly the same uptake for short times.

As time progresses, the solute will migrate deeper into the slab. Now, the approximation using spheres will not be exact. However, Neretnieks (1972) has shown that the deviation in uptake is small even at larger times. Eventually, the slab or spherical blocks will be saturated with solute, assuming that the solute flux is maintained at the inlet boundary.

Referring to the discussion above, two cases of different depth of nuclide penetration may be distinguished as "nonpenetrating" and "penetrating" cases. To exemplify this for the sphere-diffusion problem, the two following variables are defined: dimensionless radius $R' = r/r_o$ and dimensionless time $T' = D_p\varepsilon_p t/Kr_o^2$. In view of these and neglecting sources, we may rewrite (4)

$$\frac{\partial^2 c_p}{\partial R'^2} + \frac{2}{R'}\frac{\partial c_p}{\partial R'} = \frac{\partial c_p}{\partial T'} \quad . \tag{18}$$

We now subject this sphere to a uniform boundary condition of $c = c_o$ at the spherical surface. The solution to the above problem is given by (Carslaw and Jaeger, 1973):

$$c_p(R', T') = c_o\left[1 + \frac{2}{\pi R'}\sum_{n=1}^{\infty}\frac{(-1)^n}{n}\sin[n\pi R']\exp[-n^2\pi^2 T']\right] \tag{19}$$

The solution is graphically shown in Figure 4. For values of $T' < 10^{-3}$, c_p/c_o falls to less than 0.5 within 3% of r_o from the surface of the sphere. We will refer to this very early time behavior as the "nonpenetration" case.

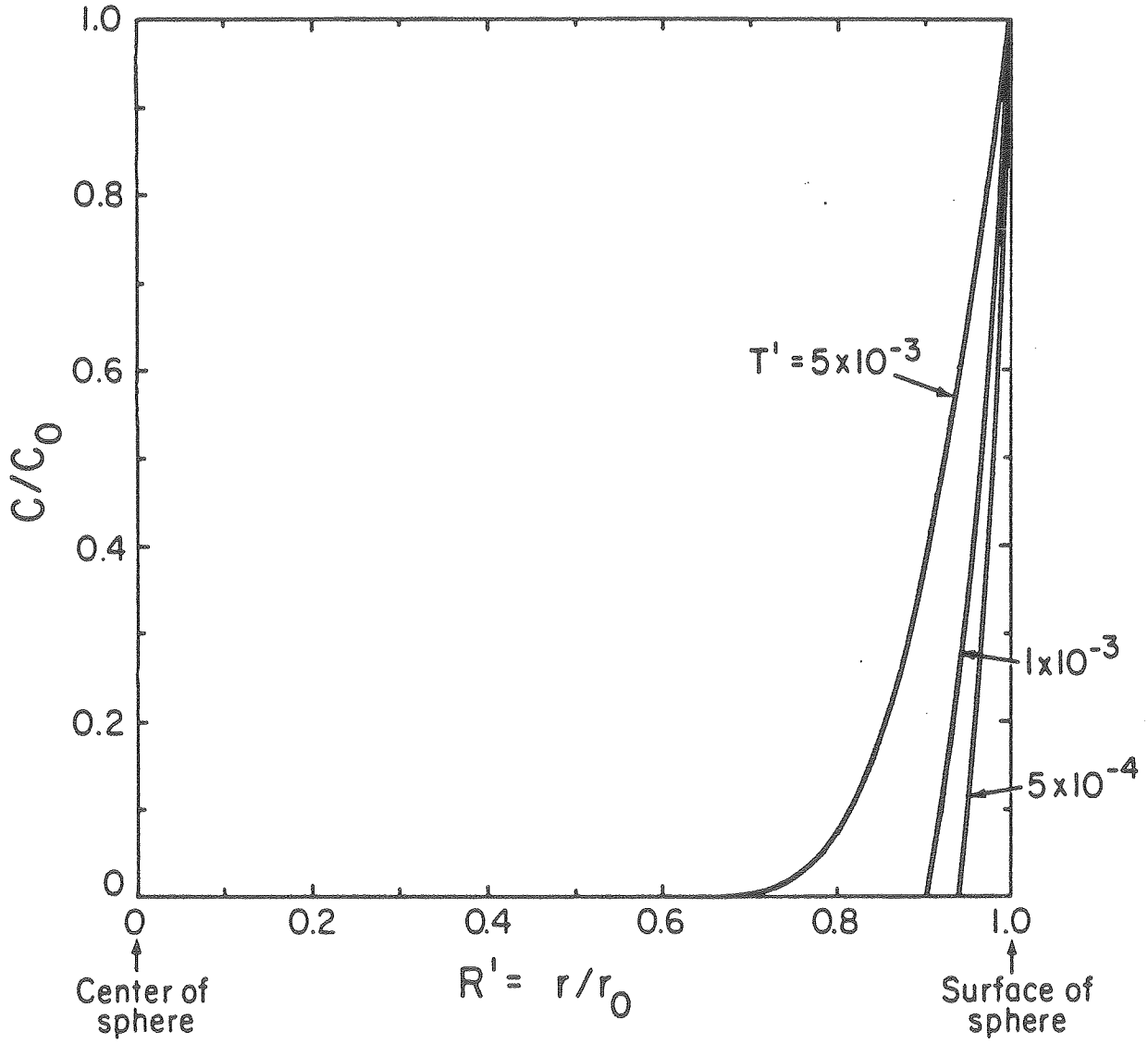

Figure 4. Diffusion in a sphere with constant surface potential c/c_o as a function of R' for various values of T'. [XBL 807-7237]

INTEGRAL FORMULATION

While the differential formulation presented above is convenient for obtaining analytic solutions, it is much simpler and less restrictive to formulate the problem in terms of integrals for purposes of numerical simulation. Consider a conveniently small volume element ℓ of the flow region (Fig. 5A) within which the average properties such as concentration vary smoothly. We shall associate the average properties over these elements with representative nodal points within the element. An element may be either the rock material or a fracture (Fig. 5B); from a theoretical point of view, the element may have any shape. Let the volume element be bounded by the closed surface Γ. Portions of Γ are interior to the flow region (Γ_i), the rest (Γ_b) coincide with the external boundary of the region. We may now write the equation of conservation of mass for the solute, incorporating advection and diffusion, as

$$-\int_{\Gamma_b+\Gamma_i} (q.n\, d\Gamma)c_\Gamma + \int_{\Gamma_b+\Gamma_i} D\nabla c.n d\Gamma - VKg_d c = VK\frac{\partial c}{\partial t} \qquad (20)$$

In equation (20), if the volume element is a fracture, $c = c_f$ and $K = 1$. If, on the other hand, the volume element is made up of the rock matrix, then the first integral in (20), denoting advection, vanishes and $c = c_p$ and $K = K_A + \varepsilon_p$. Furthermore, unlike the case with the differential equation, there is no need to specify an internal boundary condition (equation 13) for the fracture-rock interface. This interface is automatically included in the second surface integral in (20), denoting the diffusive transfer. Since we shall restrict ourselves to one-dimensional fluid flow in the fracture, we

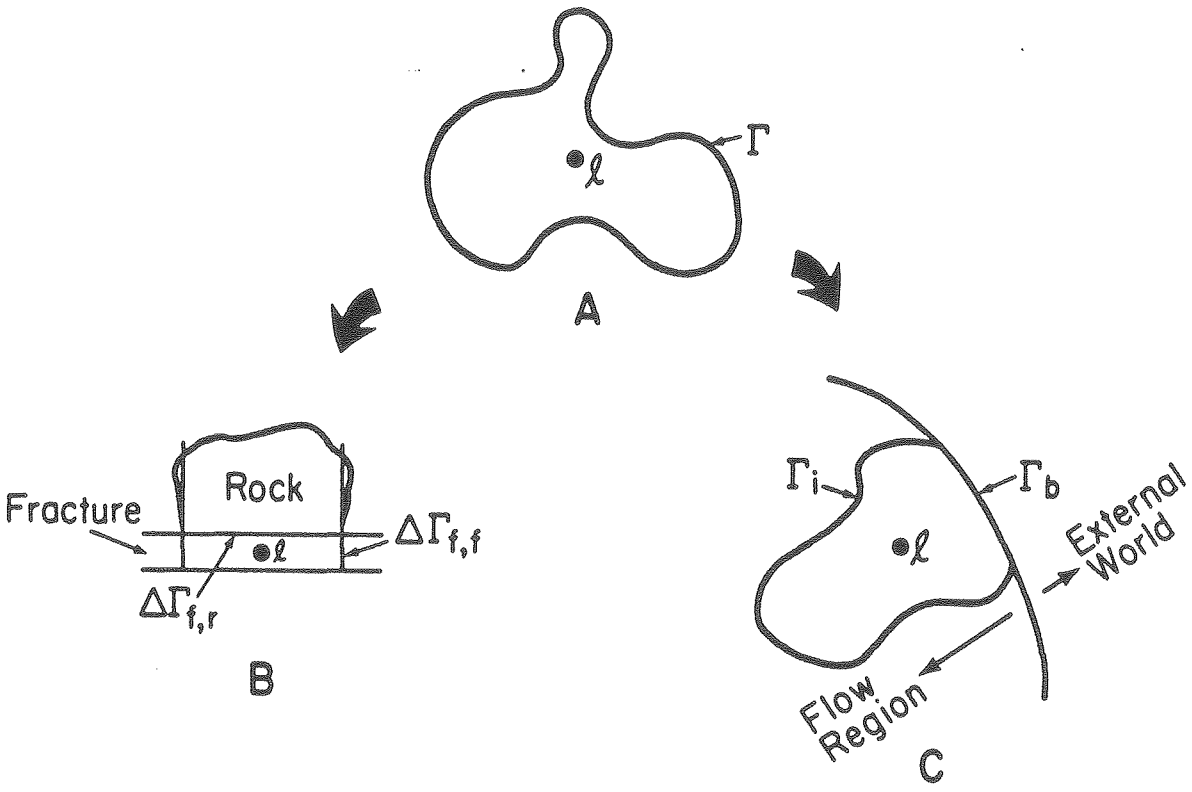

Figure 5. Definition of volume element, nodal point, interior surface segment, and boundary surface segment for the IFD scheme. [XBL 807-7236]

will consider only longitudinal diffusion (dispersion) within the fracture and set $D = D_L$ in (20) when $d\Gamma$ separates two adjoining fracture elements.

The relation of the integral equation (20) to the conventional differential equation is simple. Applying (20) to a vanishingly small volume element and normalizing it with reference to the bulk volume readily leads to (3) and (4). It is very convenient to formulate the numerical equations directly rather than integrating the differential equations (3) and (4) as suggested by Narasimhan (1978). One such direct approach, which uses the finite-difference approximation for evaluating gradients, is the Integral Finite Difference Method (IFDM) (Narasimhan and Witherspoon, 1976). We shall employ the IFDM in the present work.

NUMERICAL SCHEME

The IFD scheme used in this paper was originally developed by Edwards (1969) who incorporated it into a computer program called TRUMP. This program solves, in general, transient potential distributions in multidimensional systems with advection, conduction, and source terms. The spatial discretization allows complex geometrical configurations of volume elements. Material properties, boundary conditions, and sources may all be functions of either time or potential. For advancing in the time domain, a mixed explicit-implicit iterative scheme (Narasimhan et al., 1978) is followed. The iterative scheme consists of a Point-Jacobi type method with an acceleration factor.

Consider an arbitratily shaped, appropriately small subdomain ℓ (Fig. 6) bounded by the closed surface Γ whose average properties, such as concentration,

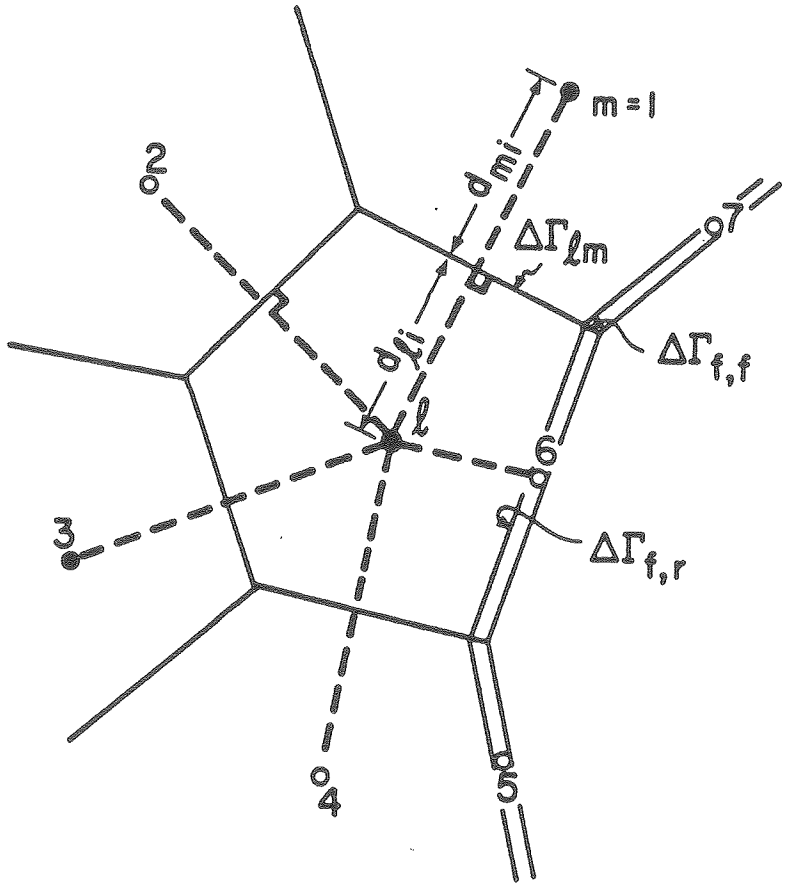

Figure 6. Schematic IFD mesh with volume element (node) ℓ in the rock matrix communicating into other rock or fracture elements. [XBL 807-7234]

are associated with an interior nodal point ℓ. Let this subdomain communicate with neighboring volume elements, designated m = 1, 2, 3, ..., such that the line joining ℓ and m is perpendicular to the interface $\Delta\Gamma_{\ell,m}$ separating the elements. Then, one may directly write the discretized form of (20) as:

$$\sum_b F_{\ell,b}\bar{c}_{\ell,b} + \sum_m F_{\ell,m}\bar{c}_{\ell,m} + \sum_b U_{\ell,b}(c_b - c_\ell)$$

$$+ \sum_m U_{\ell,m}(c_m - c_\ell) - V_\ell K\lambda_d c_\ell = V_\ell K_\ell \frac{\Delta c_\ell}{\Delta t} \qquad (21)$$

where $F_{\ell,b}$, $F_{\ell,m}$ are volumetric fluxes into element ℓ across boundary and interior surface segments, respectively, given by $F = (-\vec{q}\cdot\vec{n})d\Gamma$; $\bar{c}_{\ell,b}$, $\bar{c}_{\ell,m}$ are mean concentrations of the fluid at the boundary and interior surface segments; $U_{\ell,b}$ and $U_{\ell,m}$ are the conductances of the boundary and interior surface segments given by $U_{\ell,b} = D_{\ell,b}\Delta\Gamma_{\ell,b}/d_{\ell,b}$, $U_{\ell,m} = D_{\ell,m}(\Delta\Gamma_{\ell,m}/d_{\ell,m})$ in which $\Delta\Gamma$ is the area of cross section of the surface segment, d is the distance between nodal points, and D is the diffusivity at the appropriate interface; V_ℓ is volume of the element; K_ℓ is the equilibrium constant for the material contained in ℓ; and Δc_ℓ is the average change in concentration in element ℓ.

In the present work, steady-state fluid flow is assumed and $F_{\ell,b}$ and $F_{\ell,m}$ are a priori known. The conductances are computed based on material properties as well as the geometric quantities. The quantities, $\Delta\Gamma_{\ell,b}$, $\Delta\Gamma_{\ell,m}$, $d_{\ell,b}$, and $d_{\ell,m}$ are explicitly provided as input data for every interface in the flow region. The only other geometric parameter V_ℓ is also provided as input. Should material properties or sources vary with potential or time, appropriate estimated mean values will be used for each time step, thereby quasi-linearizing the nonlinear equation.

Ultimately, therefore, the success in solving (21) depends on the accuracy with which $\bar{c}_{\ell,b}$, $\bar{c}_{\ell,m}$, c_ℓ, and c_m can be computed for each chosen Δt, since all these quantities vary in space and in time. Let us now consider each of these terms separately.

Estimating Interface Concentration to Compute Advective Solute Transfer

Note that for computing advective solute transfer we require c at the location of the interface between adjoining volume elements. Yet, since the initial values are prescribed only at nodal-point locations, we are forced to estimate c_Γ in terms of the nodal-point concentrations in the vicinity of the interface of interest. In TRUMP, we choose to estimate the concentration at the interface $\Delta\Gamma_{\ell,m}$ by interpolating between c_ℓ and c_m, the respective values at nodal points ℓ and m. If $d_{\ell,i}$ and $d_{m,i}$ are the distances respectively from nodal points ℓ and m to the interface, then using a linear, finite-difference approximation,

$$c_{\ell,m} = \frac{d_{m,i}c_\ell + d_{\ell,i}c_m}{d_{\ell,i} + d_{m,i}} . \tag{22}$$

While this logic of interpolation is reasonably accurate for concentration profiles generated due to pure diffusion, it will yield significantly wrong estimates of $\bar{c}_{\ell,m}$ when the concentration profile is dominated by advection and is sharp, rather than diffuse. However, when the profile is only moderately dominated by advection, one could approximately account for the sharp profile by the reasoning that the interface concentration in the vicinity of the profile will be controlled to a large extent by the concentration at the node on the upstream side of the interface. This has given rise to the concept of

"upstream" or "upwind" weighting. Thus, if fluid is moving from nodal point ℓ to m, then

$$\bar{c}_{\ell,m} = \zeta c_{\ell} + (1 - \zeta)c_{m}, \qquad 0.5 < \zeta < 1.0 \tag{23}$$

where ζ is the upstream weighting factor. It should be emphasized here that the above approach is reasonable only when advection is accompanied by adequate diffusion. In problems with little or very little diffusion, upstream weighting will not yield acceptable solutions. In such problems, when ζ is closer to 0.5, the computed profile will have oscillations close to the front while if ζ is in excess of 0.7 the oscillations will be damped but the profile will be spread out as if strong diffusion were present. This phenomenon has been termed "numerical dispersion." The TRUMP program, especially designed for moderately advective problems, gives acceptable results when $\zeta = .65$. The relative importance of advection and diffusion can be quantified by the Peclet number. For a simple one-dimensional problem with uniform cross section and constant element width Δz, it is customary to define a Peclet number for the numerical problem by

$$Pe_{\ell} = \frac{1}{2}\frac{\Delta z v_f}{D} \tag{24}$$

However, in the context of the integral formulation, it is possible to give a more general, physical definition to the Peclet number. Thus the Peclet number is the ratio between the ability of the bounding surface of a volume element to advect solute into the element (advectance) to its ability to conduct solute into the element (conductance). The general definition is:

$$Pe_{\ell} = \frac{\sum_{b}^{\text{upstream}} F_{\ell,b} + \sum_{m}^{\text{upstream}} F_{\ell,m}}{\sum_{b} U_{\ell,b} + \sum_{m} U_{\ell,m}} \tag{25}$$

where Pe_{ℓ} is the Peclet number for volume element ℓ and the other symbols are as explained in (21). Note that in (25) Peclet number is given a local significance and is defined with respect to a particular volume element. Peclet number, therefore, can vary spatially within the flow region. In addition, (25) gives an invariant definition of the parameter. If we apply (25) to a one-dimensional problem of uniform cross section and nodal spacing we can easily verify that $Pe_{\ell} = v_f \Delta z/2D$.

Estimating Interface Gradient to Compute Conductive Solute Transfer

To compute the solute flux normal to an interface $d\Gamma$, we need to estimate $(\vec{q}.\vec{n}d\Gamma)$. For this in the IFDM, we use the finite-difference approximation, subject to the condition that the line joining nodal points ℓ and m is normal to the interface $\Delta\Gamma_{\ell,m}$ separating the volume elements ℓ and m. Thus the flux of solute is given by $[D\Delta\Gamma_{\ell,m}(c_m - c_{\ell})]/d_{\ell,m} = U_{\ell,m}(c_m - c_{\ell})$.

The Discretized Equations

In view of the foregoing, the discretized equation (21) for the advective diffusion problem may be rewritten as

$$\sum_{b} F_{\ell,b}\bar{c}_{\ell,b} + \sum_{m} F_{\ell,m}\bar{\bar{c}}_{\ell,m} + \sum_{b} U_{\ell,b}(\bar{c}_b - \bar{c}_{\ell})$$

$$+ \sum_{m} U_{\ell,m}(\bar{c}_n - c_{\ell}) - V_{\ell}K\lambda_d c_{\ell} = V_{\ell}K_{\ell}\frac{\Delta c_{\ell}}{\Delta t} \tag{26}$$

In the IFDM algorithm, the steady fluxes, $F_{\ell,m}$, $F_{\ell,b}$, the boundary potentials $c_{\ell,b}$, c_b as well as the geometric parameters needed to compute $U_{\ell,m}$, $U_{\ell,b}$, and V_ℓ are all provided as input data. In order to solve (26), therefore, we need only to consider the mean nodal concentrations $\bar{c}_\ell$, $\bar{c}_m$ and the mean interface concentration $\bar{\bar{c}}_{\ell,m}$. Since these concentrations are all functions of time, it is necessary to define these time-averaged means. Indeed, it is clear that these averages should satisfy the following relations

$$U_{\ell,m}(\bar{c}_m - \bar{c}_\ell) = \frac{1}{\Delta t}\int_{t_o}^{t_o+\Delta t} U_{\ell,m}(c_m - c_\ell)\, dt \tag{27}$$

and

$$F_{\ell,m}\bar{\bar{c}}_{\ell,m} = \frac{1}{\Delta t}\int_{t_o}^{t_o+\Delta t} F_{\ell,m}\bar{c}_{\ell,m}\, dt \tag{28}$$

Note that in (28) $\bar{\bar{c}}_{\ell,m}$ denotes a mean value in space and in time while $\bar{c}_{\ell,m}$ is only a spatial mean.

In order to satisfy (27) we shall let $\bar{c}_i = c_i^o + \theta\Delta c_i$, $i = \ell, m$, in which $0 < \theta < 1.0$. For unconditional stability, $0.5 < \theta < 1.0$. In order to satisfy (28), in vies of (23) we may write

$$\bar{\bar{c}}_{\ell,m} = \zeta(c^o_{up} + \theta\Delta c_{up}) + (1 - \zeta)(c^o_{down} + \theta\Delta c_{down})$$

$$= [\zeta c^o_{up} + (1 - \zeta)c^o_{down}] + \theta[\zeta\Delta c_{up} + (1 - \zeta)\Delta c_{down}] \tag{29}$$

However, in the TRUMP code, Edwards (1969) modified (29) slightly and set $\zeta = 1$ in the terms associated with θ in (29) to get

$$\bar{\bar{c}}_{\ell,m} = [\zeta c^{o}_{up} + (1 - \zeta)c^{o}_{down}] + \theta\Delta c_{up}] \tag{30}$$

Edwards (personal communication) devised (30) primarily to combine the advantages of variable θ in the explicit part with unconditional stability in the implicit solution. In (26) if we set $\theta = 0$, we get the following explicit relation,

$$\Delta c_{\ell,exp} = \frac{\Delta t}{V_\ell K_\ell}\left\{\sum_b F_{\ell,b}c_{\ell,b} + \sum_m F_{\ell,m}[c^{o}_{up} + (1 - \zeta)c^{o}_{down}]\right.$$

$$\left. + \sum_b U_{\ell,b}(c_b - c^{o}_{\ell}) + \sum_m U_{\ell,m}(c^{o}_{m} - c^{o}_{\ell}) - V_\ell K\lambda_d[c^{o}_{\ell} + \theta\Delta c_{\ell,est}]\right\} \tag{31}$$

It is well known that the explicit equation (or forward differencing equation) will violate the maximum principle and give rise to unstable oscillations if Δt exceeds a critical limit, definable for each volume element. Physically, this critical limit or the "stable time step" for a volume element is the ratio of its capacity to sorb solute to the sum of the conductances and advectances across its bounding surface. Thus,

$$\Delta t_{stab,\ell} = \frac{V_\ell K_\ell}{\sum_b U_{\ell,b} + \sum_m U_{\ell,m} + \sum_m^{upstream} F_{\ell,m}} \tag{32}$$

Therefore, for $\Delta t > \Delta t_{stab,\ell}$, (31) cannot be applied to compute Δc_ℓ. It can be shown that for unconditional stability, when $\Delta t > \Delta t_{stab,\ell}$, $0.5 < \theta < 1.0$. In view of this and the definition of c_ℓ, c_m and $c_{\ell,m}$ we may write,

$$\Delta c_{\ell} = \frac{\Delta t}{V_{\ell} K_{\ell}} \left(\sum_{b} F_{\ell,b} c_{\ell,b} + \sum_{m} F_{\ell,m} \left[\zeta c^{o}_{up} + (1 - \zeta) c^{o}_{down} + \theta \Delta c_{up} \right] \right.$$

$$+ \sum_{b} U_{\ell,b} \left[c_{b} - \left(c^{o}_{\ell} + \theta \Delta c_{\ell} \right) \right] + \sum_{m} U_{\ell,m} \left[\left(c^{o}_{m} + \theta \Delta c_{m} \right) - \left(c^{o}_{\ell} + \theta \Delta c_{\ell} \right) \right]$$

$$\left. - V_{\ell} K \lambda_{d} \left(c^{o}_{\ell} + \theta \Delta c_{\ell} \right) \right) . \qquad (33)$$

Using the expression for $\Delta c_{\ell,exp}$ given in (31) we may simplify (33) to

$$\Delta c_{\ell} = \Delta c_{\ell,exp} + \frac{\theta \Delta t}{V_{\ell} K_{\ell}} \left(\sum_{m} F_{\ell,m} \Delta c_{up} - \sum_{b} U_{\ell,b} \Delta c_{\ell} + \sum_{m} U_{\ell,m} (\Delta c_{m} - \Delta c_{\ell}) \right) \qquad (34)$$

In (34), if $\theta = 0.5$ we get the well-known Crank-Nicolson or central-differencing scheme, while $\theta = 1$ leads to the fully implicit backward-differencing scheme. In TRUMP, θ is a function of time and is recomputed for every time step such that $0.57 < \theta < 1.0$ (for details see Edwards (1969) or Narasimhan et al. (1978). The set of equations for Δc_{ℓ}, $\ell = 1, 2, 3, \ldots, L$, where L is the total number of volume elements in the system at which Δc has to be evaluated, is obviously an implicit set since Δc occurs on both sides of the equation. They could be solved either directly using successive elimination or related techniques or indirectly through iterative methods. In TRUMP, the iterative approach is used, using a mixed explicit-implicit scheme (Narasimhan et al., 1978). The basic philosophy of this approach is that since Δt_{stab} varies from element to element, the implicit computations are needed only for those elements for which $\Delta t > \Delta t_{stab}$. Looking at the form of (34), it is easy to see that all the terms except $\Delta c_{\ell,exp}$ on the right-hand side need to be computed only for those volume elements whose stability limit is exceeded by

the current time step. For a detailed description of the iterative scheme the reader is referred to the TRUMP manual by Edwards (1969). Briefly, the iterative procedure consists in the following substitutions vis-a-vis (34):

$$\Delta c_\ell(\text{left side}) = \Delta c_\ell^{p+1} \tag{35a}$$

$$\Delta c_\ell(\text{right side}) = (1 + g)\Delta c_p^{p+1} - g\Delta c_\ell^{p} \tag{35b}$$

$$\Delta c_m(\text{right side}) = \Delta c_m^{p} \tag{35c}$$

where the superscript p is the iteration number and g is an acceleration factor, whose optimal value appears to be 0.2. For $p = 0$, Δc_ℓ^p and Δc_m^p are carefully calculated estimates based on past system behavior.

RESULTS

The TRUMP model was applied to the following five test problems:

1. One-dimensional transport with advection and dispersion in a uniform fracture.

2. Advection and dispersion in a set of parallel fractures with diffusion in microfissured matrix: Early time solution.

3. Advection and dispersion in a set of parallel fractures with diffusion in microfissured matrix: Solution for large times.

4. Case 2 with radioactive decay.

5. Case 3 with radioactive decay.

The results of these applications are discussed below. The parameters used in the problems are summarized in Table 1.

Table 1. Parameters used in the problems.

Parameter	Dimension	Problem Number 1	2	3	4	5
Fluid Velocity, v_f	m/s.	4.1×10^{-6}	4.0717×10^{-6}	3×10^{-7}	4.0717×10^{-6}	3×10^{-7}
Fluid Flux, F	$m^3/m.s$	1.52×10^{-10}	1.5×10^{-10}	3×10^{-12}	1.5×10^{-10}	3×10^{-12}
Long. Dispersion-Coefficient in Fracture, D_L	m^2/s	10^{-5} to 10^{-10}	10^{-5}, 10^{-7}	1.35×10^{-4}	10^{-5}	1.35×10^{-4}
Fracture Spacing, S	m	--	50	1.0	50	1.0
Fracture Porosity, ε_f		--	7.368×10^{-7}	10^{-5}	7.368×10^{-7}	10^{-5}
Radius of Sphere, r_o	m	--	75	1.5	75	1.5
Volume of Equilibrium Constant, K	m^3/m^3	1.0	10^4	10^4	10^4	10^4
Effective Diffusivity in Bulk Solid, $D_p\varepsilon_p$	m^2/s	--	10^{-12}	10^{-12}	10^{-12}	10^{-12}
Decay Constant, λ_d	1/s	--	--	--	8.6643×10^{-7} 8.6643×10^{-8}	7.335×10^{-17}
Fracture Aperture, 2b	m	3.7×10^{-5}	3.684×10^{-5}	10^{-5}	3.684×10^{-5}	10^{-5}
Hydraulic Conductivity of fissure, K_f	m/s	1.12×10^{-3}	1.36×10^{-3}	1.00×10^{-4}	1.36×10^{-3}	1.00×10^{-4}
Hydraulic Conductivity of bulk rock, K_r	m/s	--	10^{-9}	10^{-9}	10^{-9}	10^{-9}
Hydraulic Gradient, i	m/m	3.66×10^{-3}	3×10^{-3}	3×10^{-3}	3×10^{-3}	3×10^{-3}
Length of Fracture Element, Δz	m	0.05 to 0.5	0.025 to 0.20	15 to 100	0.025 to 0.20	15 to 100

Problem 1: One-dimensional Transport in a Single Fracture

The first problem was set up to study the effect of Peclet number and upstream weighting factor on numerical dispersion. Consider a fracture with an aperture of 3.7×10^{-5} m and length 5 m through which water flows at a constant velocity of 4.1×10^{-6} m/s corresponding to a volumetric flux of 1.52×10^{-10} $m^3/m,s$. Longitudinal dispersion in the fracture, D_L is assumed to vary between 10^{-5} and 10^{-10} m^2/s. At $t = 0$, water enters with a constant concentration of c_o, while the initial concentration everywhere in the fracture is 0. It is required to compute c_f as a function of space and time. The analytical solution to the above problem is well known (e.g. Fried and Combarnous, 1971) and is given by

$$\frac{c_f}{c_o}(z, t) = \frac{1}{2}\left(\operatorname{erfc}\left[\frac{z - v_f t}{2(D_L t)^{1/2}}\right] + \exp\left(\frac{v_f z}{D_L}\right)\operatorname{erfc}\left[\frac{z + v_f t}{2(D_L t)^{1/2}}\right]\right) \quad (36)$$

Several numerical experiments were performed with the fracture divided into uniform volume elements with Δz varying from 0.05 to 0.5 m. Defining a Peclet number as in (24), it was found that stable solutions were obtained for Pe_ℓ less than approximately 2. Also, for values of $Pe_\ell < 2$, accuracy was found to increase with decreasing Pe_ℓ.

A comparison of the numerical results with the analytic solution is presented in Figures 7 through 9. Figure 7 shows the effect of upstream weighting at a given $Pe_\ell = 10.25$. It is readily seen that severe oscillations occur at low upstream weight factors. At higher upstream weights the oscillations are damped but the profile is smeared out. The effect of varying Pe at a constant

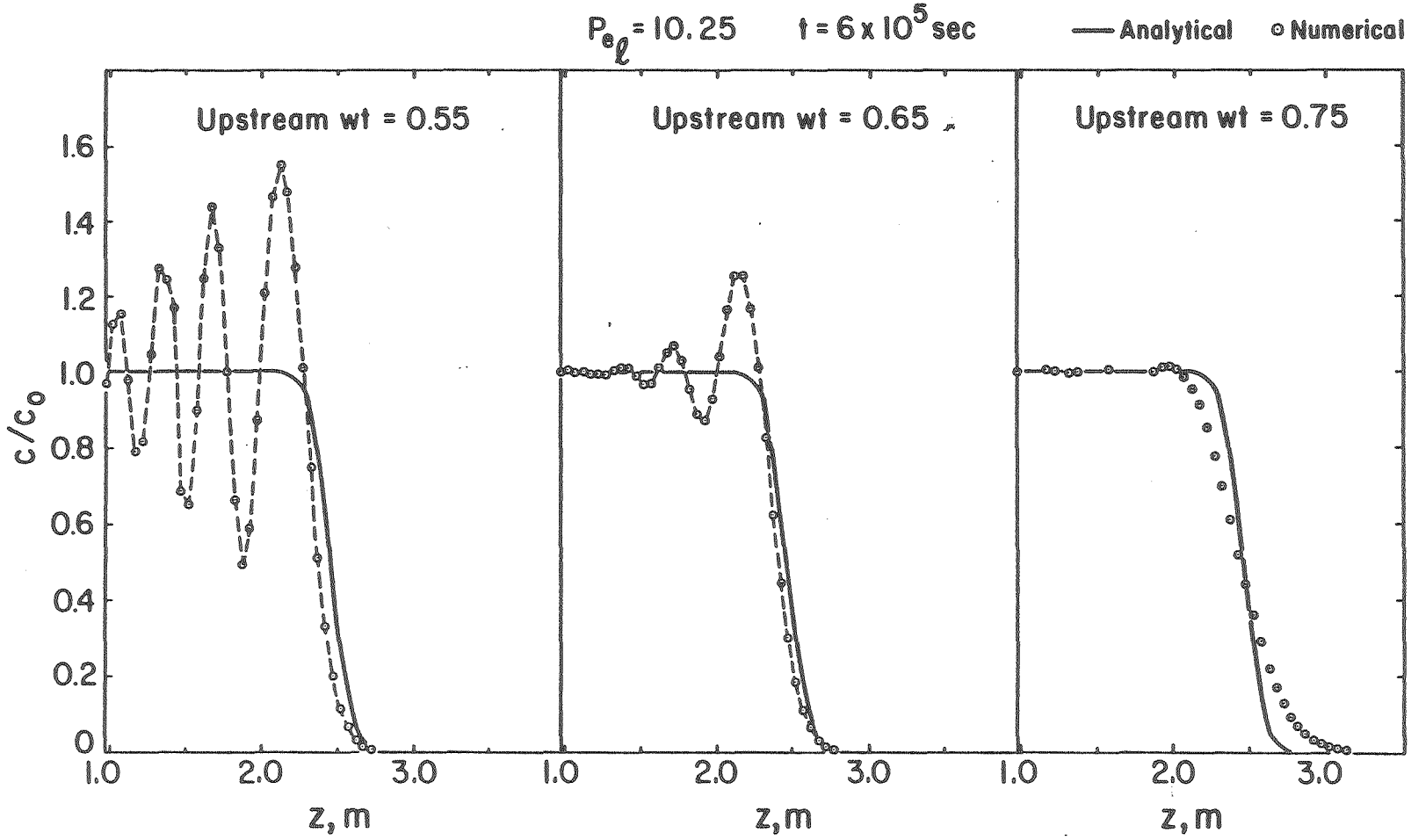

Figure 7. One-dimensional advection-diffusion problem: Effect of upstream weighting at Pe_ℓ = 10.25. [XBL 807-7238]

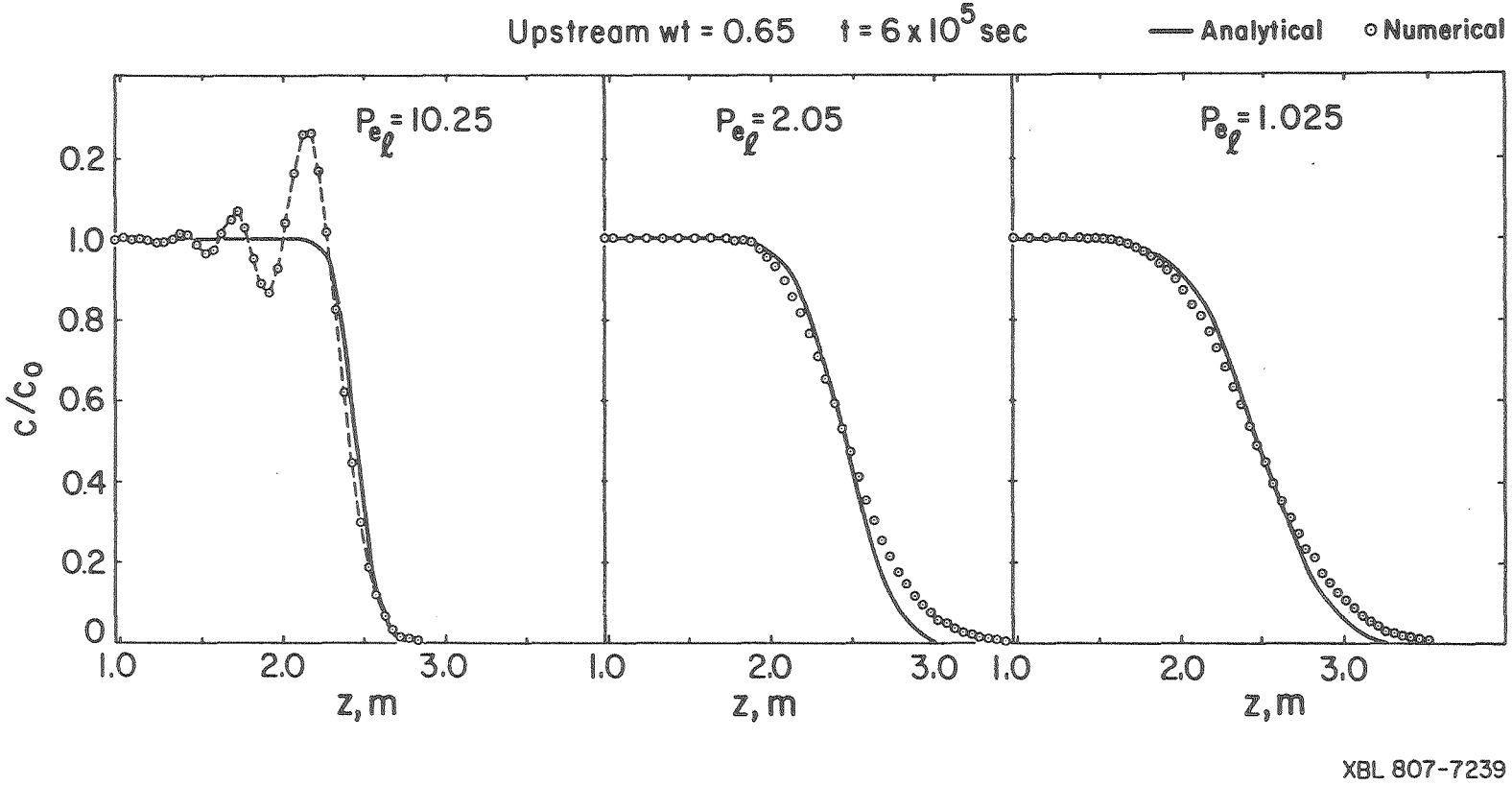

Figure 8. One-dimensional advection-diffusion problem: Effect of Peclet Number at $\zeta = 0.65$.
[XBL 807-7239]

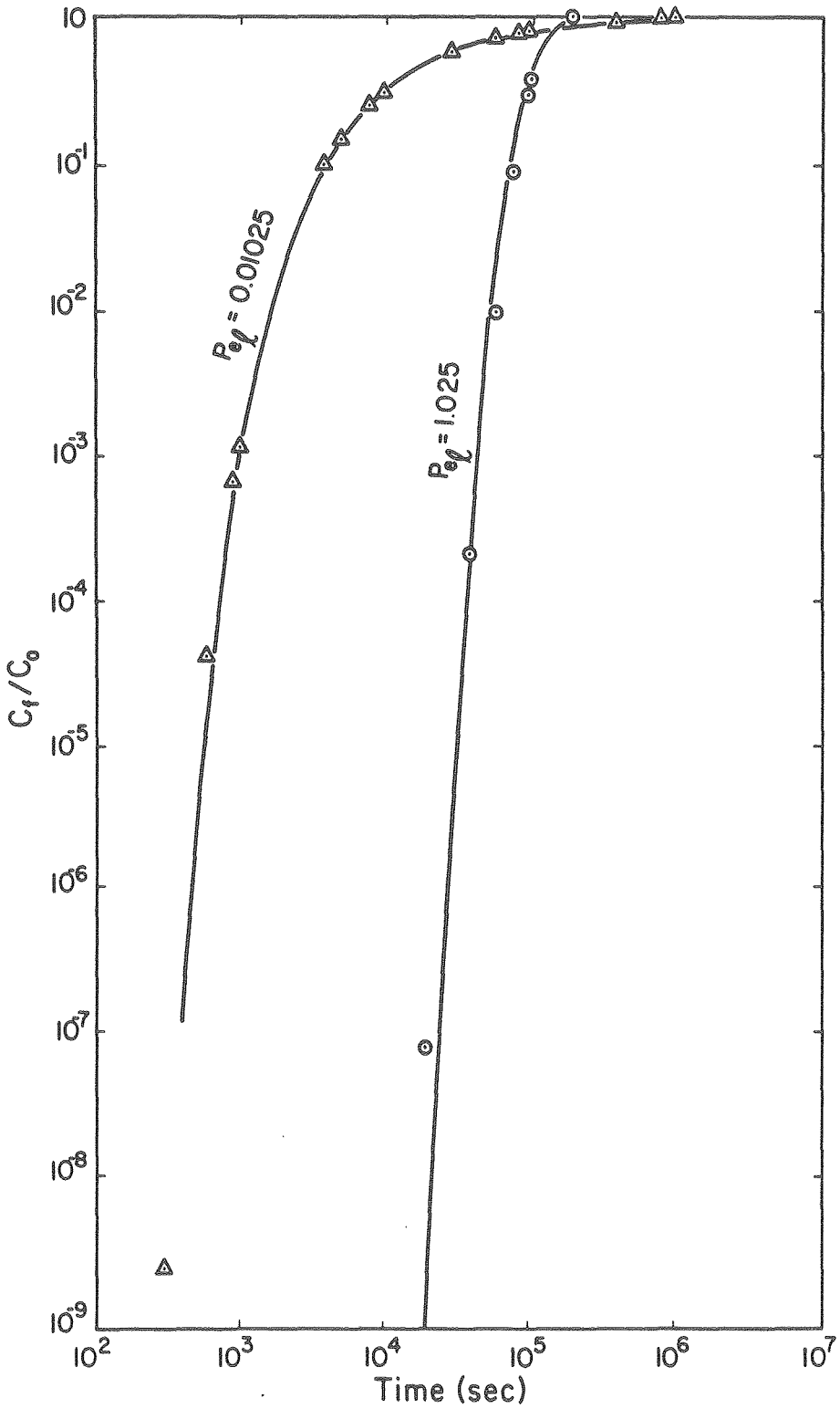

Figure 9. One-dimensional advection-diffusion problem: Comparison of breakthrough curves with solution for two different Peclet Numbers.

[XBL 807-7240]

upstream weight is seen in Figure 8. It is seen that stable solutions are obtained for Pe_ℓ less than 2 and that accuracy is inversely related to Pe_ℓ. The purpose of Figure 9 is to indicate the type of accuracy that one could obtain when Pe_ℓ is appropriately small. The breakthrough curves at z = 0.475 m are given. It is seen that as Pe_ℓ decreases below 1 accuracies of 1 part in 10^6 are quite attainable.

Problem 2 Advective-Dispersion in Parallel Fractures with Diffusion in Rock Matrix: Early Time Solution (Nonpenetrating Case)

Consider the geometry in Figure 3. A set of parallel horizontal fractures with aperture $2b = 3.684 \times 10^{-5}$ m are spaced 50 m apart. Within the fracture, fluid moves at a constant velocity of 4.0717×10^{-6} m/s. Assuming that flow in the fracture obeys cubic law (Witherspoon et al., 1980), this translates to a permeability of approximately 0.1 md for the bulk rock and a hydraulic gradient of 3×10^{-3} m/m. The fracture porosity ε_f of the rock is 7.368×10^{-7}. The volume equilibrium constant $K = 10^4$ m^3/m^3. The effective diffusivity of the bulk solid, $D_p\varepsilon_p = 10^{-12}$ m^2/s while two different values of longitudinal dispersion $D_L = 10^{-5}$ and 10^{-7} m^2/s were used.

The analytical solution to this problem was obtained by assuming that the rock slabs are replaced by spheres having the same surface to volume ratio as the slabs. As discussed in the section on "Depth of Nuclide Penetration," this approximation is very good at early times. The system can be represented by the following differential equations:

$$-v_f \frac{\partial c_f}{\partial z} + D_L \frac{\partial^2 c_f}{\partial z^2} - w = \frac{\partial c_f}{\partial t} \tag{37}$$

$$D_p \varepsilon_p \left[\frac{\partial^2 c_p}{\partial z^2} + \frac{2}{r} \frac{\partial c_p}{\partial r} \right] = K \frac{\partial c_p}{\partial t} \tag{38}$$

subject to the boundary conditions

$$c_f(0, t) = c_o \tag{39}$$

$$c_f(\infty, t) = 0 \tag{40}$$

$$c_f(z, 0) = 0 \tag{41}$$

$$\frac{\partial c_p}{\partial r}(0, z, t) = 0 \tag{42}$$

$$c_p(r_o, z, t) = c_p\Big|_{r=r_o}, \text{ given by } w = \frac{1 - \varepsilon_f}{\varepsilon_f} \frac{3k_f}{b} (c - c_p)\Big|_{r=r_o} \tag{43}$$

$$c_p(r, z, 0) = 0 \tag{44}$$

where k_f is a mass transfer coefficient.

The boundary condition (43) is the link between equations (37) and (38). It states mathematically that the mass entering or leaving the particles must equal the flow of mass transported across a stagnant fluid film at the external surface. For high values of the mass transfer coefficient k_f, $c \sim c_p|_{r=r_o}$.

Equations (37) and (38) have been simultaneously solved using analytical techniques by Rasmuson and Neretnieks (1980). The solution in terms of dimensionless parameters is given by

$$\frac{c_f}{c_o} = \frac{1}{2} + \frac{2}{\pi}\int_0^{\infty} \exp\left(\frac{1}{2}\,Pe - \sqrt{\frac{\sqrt{(z^2x')^2 + (z^2y')^2} + z^2x'}{2}}\right)$$

$$\times \sin\left(y\lambda^2 - \sqrt{\frac{\sqrt{(z^2x')^2 + (z^2y')^2} - z^2x'}{2}}\right)\frac{d\lambda}{\lambda} \tag{45}$$

with

$$z^2x' = Pe\left(\frac{1}{4}\,Pe + \delta H_1\right) \tag{46}$$

$$z^2y' = \delta Pe\ \frac{2}{3}\frac{\lambda^2}{R} + H_2 \tag{47}$$

$$H_1(\lambda, \nu) = \frac{H_{D_1} + \nu\left(H_{D_1}^2 + H_{D_2}^2\right)}{(1 + \nu H_{D_1})^2 + (\nu H_{D_2})^2} \tag{48}$$

$$H_2(\lambda, \nu) = \frac{H_{D_2}}{(1 + \nu H_{D_1})^2 + (\nu H_{D_2})^2} \tag{49}$$

$$H_{D_1}(\lambda) = \lambda\left(\frac{\sinh 2\lambda + \sin 2\lambda}{\cosh 2\lambda - \cos 2\lambda}\right)^{-1} \tag{50}$$

$$H_{D_2}(\lambda) = \lambda\left(\frac{\sinh 2\lambda - \sin 2\lambda}{\cosh 2\lambda - \cos 2\lambda}\right)^{-1} \tag{51}$$

and

$$Pe = v_f/D, \tag{52}$$

where Pe is a "global" Peclet number as opposed to the "local" Peclet number Pe_χ defined in equations (24) and (25). It was shown in Rasmuson and

Neretnieks (1981) that the radial concentration gradients in the fissures should be completely negligible. It follows that the film resistance is approximately 0 and H_1 and H_2 are simplified to

$$H_1(\lambda,\nu) = H_{D_1}(\lambda) \tag{53}$$

$$H_2(\lambda,\nu) = H_{D_2}(\lambda) \tag{54}$$

Note that for a sphere the specific surface is given by the relation $A/V = 3r_o$ while for an infinite slab $A/V = 2/S$, where S is fracture spacing. Hence r_o in the present case equals 75 m. We now recall that the dimensionless time T' for a sphere is $D_p\varepsilon_p t/Kr_o^2$ and $T' = 1.778 \times 10^{-20}t$ if t is in seconds, or $5.6064 \times 10^{-13}t$ if t is in years. If $t = 10^8$ years, T' equals 5.6064×10^{-5} which is extremely small. In view of Figure 4, for such a small T', the solute penetration into the matrix should be very small. In other words the system could be treated as nonpenetrating for times of up to 10^8 years or more.

The nonpenetrating case was investigated numerically with a mesh in which the rock blocks were divided into rectangular elements of length Δz and width 2d, as shown in Figure 10. Using the design of mesh shown in Figure 10, a number of runs were made with various mesh widths. A major emphasis in making the runs was to gain an understanding of the role of mesh discretization on accuracy. Recall that in radioactive waste disposal studies there may be a need to predict the early part of the breakthrough curve with a great deal of relative accuracy.

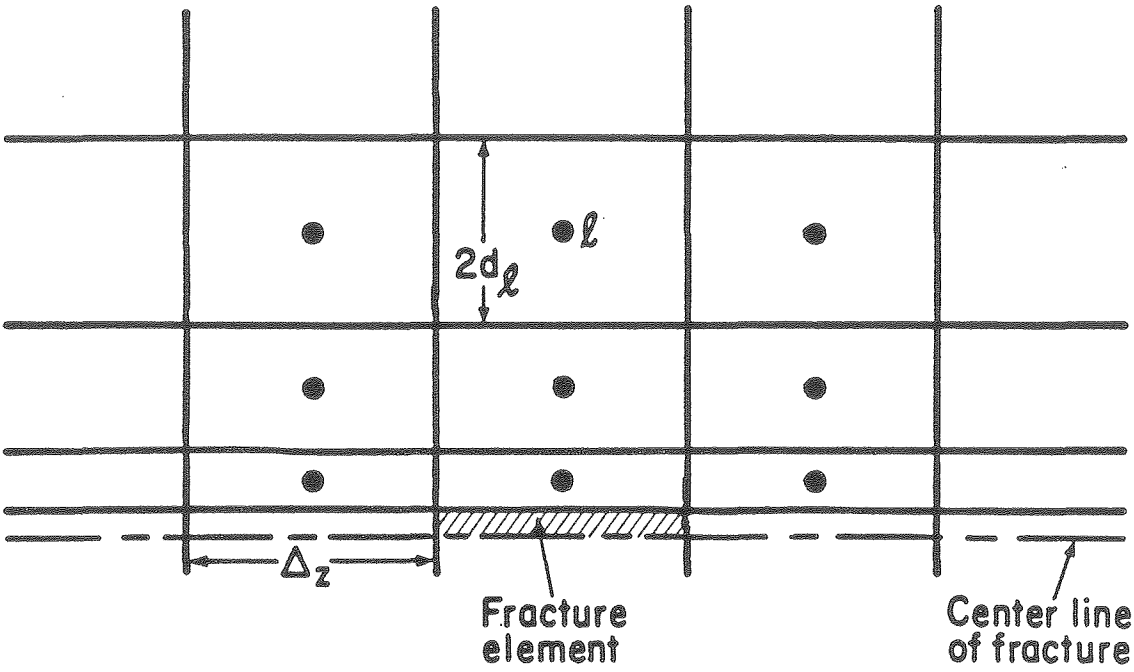

Figure 10. Schematic mesh design for advective-diffusion problem, nonpenetration case. [XBL 807-7235]

In constructing the mesh for a particular numerical problem, then, it is necessary to decide upon (a) the width of the smallest element adjacent to the fracture and (b) the rate at which the mesh shall become coarser as we proceed away from the fracture.

In this context, the capacity of a volume element immediately adjoining the fracture can be expressed by

$$\bar{C}_1 = 2K\Delta z d_1 \tag{55}$$

and the total conductance of its surfaces is given by

$$Z_1 = \frac{D\Delta z[2d_1 + d_2]}{d_1[d_1 + d_2]} \tag{56}$$

In arriving at (56), the assumption is made that there is no diffusion in the z direction within the rock matrix. For high accuracy, the volume element adjacent to the fracture should be sufficiently small so that it will react rapidly to the concentration pulse originating in the fracture. In other words it should have a reasonably small time constant or stability limit given by $\tau = \bar{C}_1/Z_1$. One simple way of investigating this is to state that if T is the first arrival of the concentration front at a given point, then τ should equal αT with α considerably less than 1. To get a reasonable number of elements in the rock matrix we will design the mesh in such a fashion that the mesh width increases by a factor β in the direction perpendicular to z. That is, $d_2 = \beta d_1$, $d_3 = \beta d_2$, and so on with $\beta > 1$.

The numerical experiments carried out indicated that good results were obtained for $0.001 < \alpha < 0.1$. When α was less than 0.001 the time constants

varied so widely over the flow region that convergence of the iterative scheme was too slow and led to inaccuracies. When α was greater than 0.1 the matrix did not react fast enough to the pulse. It was also found that $1 < \beta < 2$ gave best results. Values of $\beta > 2$ had the effect of creating large differences in time constants over the flow region, leading to slow convergence and inaccuracies.

The results of the numerical experiments are given in the form of c_f/c_o versus time at $z = 0.475$ m. Figures 11 and 12 are for two different global Peclet numbers. Figure 11 pertains to the case with $Pe = 0.19341$ in which the fracture was divided into 30 volume elements increasing in size from the inlet as 0.025 m (10), 0.05 m (10), and 0.2 m (10). Because of the variations in Δz, Pe_ℓ is, of course, variable within the flow region. The matrix was divided into 19 volume elements in the direction perpendicular to z with 10^{-5} m (4) and then increasing in size with $\beta = 1.7$. Figure 12 pertains to the case in which $Pe = 19.341$ and the fracture is discretized in the same manner as before but the matrix is divided into 24 nodes with width 10^{-6} m (4), then increasing with $\beta = 1.6$ (4) and finally increasing with $\beta = 1.7$. Note that in both the cases the agreement between the analytic and numerical solutions is good.

In radionuclide migration problems a nuclide which at no time reaches the biosphere with a concentration of 10^{-9} times that in the repository, may be considered to have decayed to insignificance (Neretnieks, 1980). For the case with $Pe = 19.341$, that is, with $D_L = 10^{-7}$ m^2/s, the relative concentration reaches 10^{-9} at $z = 0.475$ m after approximately 25 years. This should be compared with the corresponding time for the advance of the hydrodynamic front

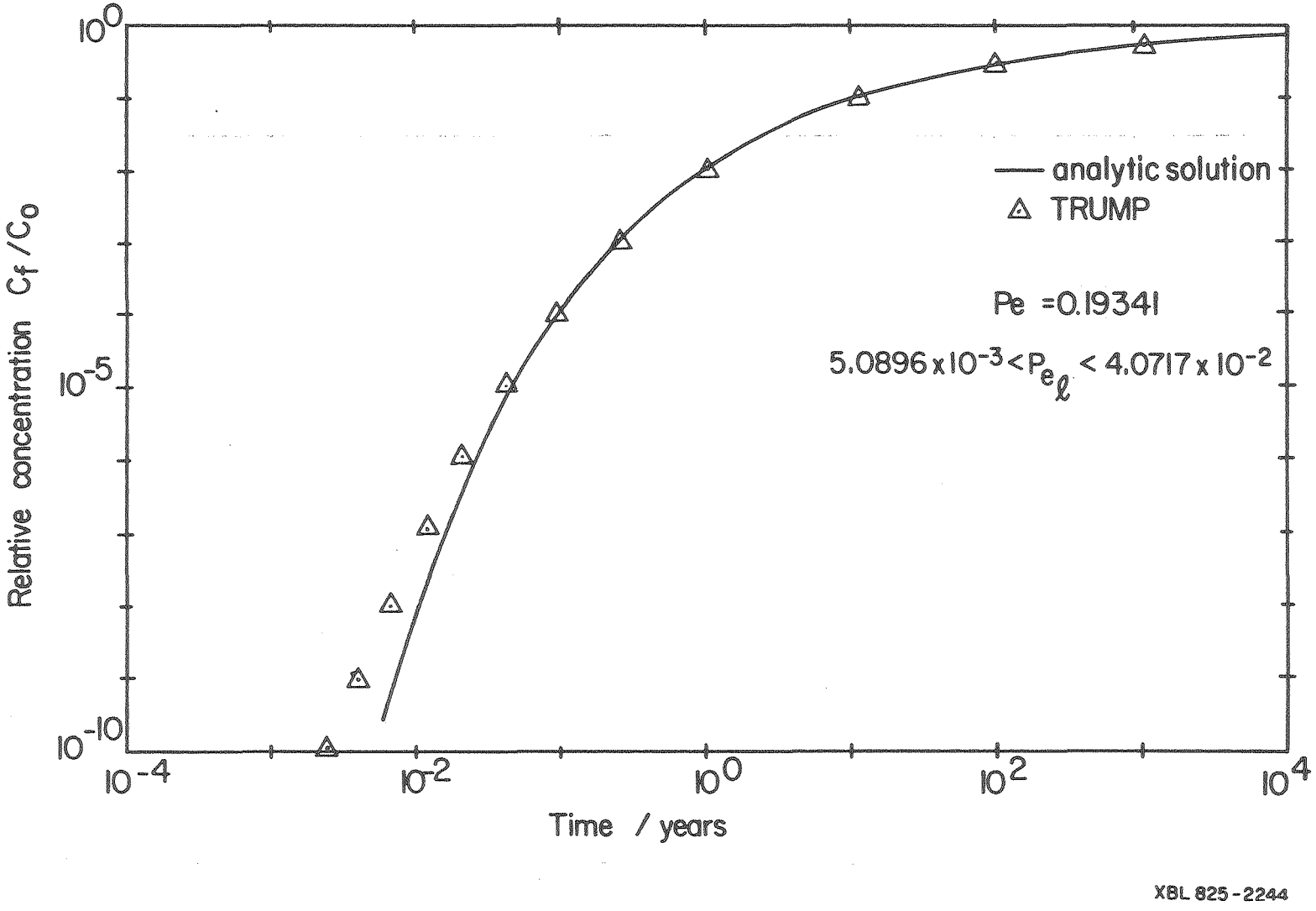

Figure 11. Nonpenetrating case: Comparison of analytic and numerical solutions for $0.005 < Pe_\ell < 0.041$ and Pe = .19341. [XBL 825-2244]

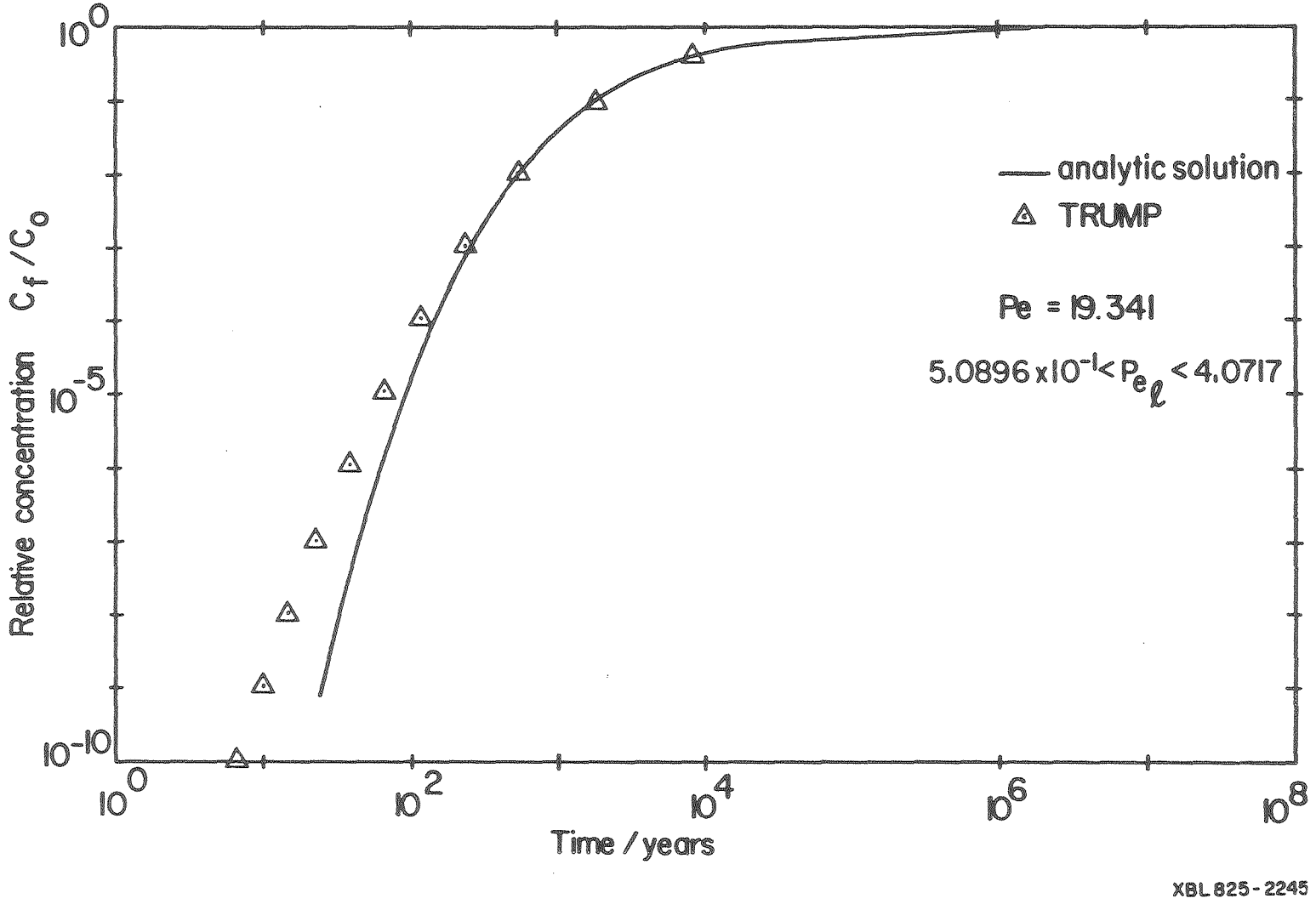

Figure 12. Nonpenetrating case: Comparison of analytic and numerical solutions for a mesh with $0.5 < Pe_\ell < 4$ and Pe = 19.341.
[XBL 825-2245]

which is only a little more than a day. When $D_L = 10^{-5}$ m^2/s (Pe = 0.19341), the relative concentration attains 10^{-9} at z = 0.475 m after only 3 days.

The implication of these two cases in the migration of radionuclides is obvious. With low magnitudes of the longitudinal dispersion, diffusion into the rock matrix has greatly helped in retarding the solute front behind the hydrodynamic front. However, longitudinal dispersion effects of larger magnitudes in the fracture can significantly diminish the retardation effects of matrix diffusion. An understanding of the relative magnitudes of the diffusion-sorption on the one hand and dispersion mechanisms on the other is therefore essential for the prediction of the migration of radionuclides from a final respository of radioactive waste. A first attempt in this direction was done by Neretnieks (1980) and Rasmuson and Neretnieks (1981).

Problem 3 Advection-Dispersion in a Set of Parallel Fractures with Diffusion in Microfissured Matrix: Large-time Solution (Penetrating Case).

In the previous example the fracture spacing was so large that penetration depth of the solute into the rock matrix was very small. However, when S becomes small, the diffusion fronts from adjacent fractures will eventually meet. For example, consider a fracture spacing of 1 m, which leads to $r_o = 1.5$ m. In this case, $T' = 1.4016 \times 10^{-9}t$, if t is in years. That is, $t = 10^6$ years now corresponds to a $T' = 1.4016 \times 10^{-3}$. In this case we would need to model radial diffusion into the spherical particles for $t > 10^6$ years.

Consider now the following set of conditions: $S = 1.0$ m, $K = 10^4$ m^3/m^3, $D_p\varepsilon_p = 10^{-12}$ m^2/s, $D_L = 1.35 \times 10^{-4}$ m^2/s, $v_f = 3 \times 10^{-7}$ m/s, $2b = 10^{-5}$ m, $\varepsilon_f = 10^{-5}$, and $r_o = 1.5$ m. For the aperture and the v_f used, the hydraulic gradient is 0.003 m/m.

In the actual simulation using TRUMP only one-half of the fracture and one-half of the adjoining rock matrix needs to be modeled because of symmetry. Hence, the actual fluid flux in the fracture equals 1.5×10^{-12} $m^3/m.s$.

We now have to decide upon the number of spherical particles over Δz. For this purpose we make use of the fracture porosity, ε_f as follows:

$$V_b = \frac{1}{2} S\Delta z \tag{57}$$

The volume of hemisphere of radius r_o is

$$V_p = \frac{2\pi}{3} r_o^3 = \frac{2\pi}{3} (1.5S)^3 \tag{58}$$

Let n be the required number of spherical particles. Thus $nV_p = V_b - V_f = V_b(1 - \varepsilon_f)$. Therefore,

$$n = \frac{V_b}{V_p} (1 - \varepsilon_f) = \frac{\Delta z(1 - \varepsilon_f)}{4.5\pi S^2} \cong \frac{\Delta z}{4.5\pi S^2} \tag{59}$$

In the TRUMP simulation, the particles were modeled in the spherical coordinate system. The volume of a differential volume element bounded by orthogonal surfaces of a spherical coordinate system with distance from the origin r, angle in the x-y plane θ, and angle from the positive z axis ϕ is given by

$$\Delta V = r^2 \sin\phi \Delta r \Delta\theta \Delta\phi \tag{60}$$

For a finite volume element or node, this becomes

$$V_\ell = \frac{1}{3}(r_2^3 - r_1^3)(\cos\phi_1 - \cos\phi_2)(\theta_2 - \theta_1) \tag{61}$$

or

$$V_\ell = 4\pi\bar{r}^2(r_2 - r_1)\left[\sin\frac{\bar{\phi}}{2}\right](\phi_2 - \phi_1)\left[\frac{\theta_2 - \theta_1}{2\pi}\right] \tag{62}$$

$$\bar{r} = r_{av}\left\{1 + \frac{1}{12}\left[\frac{r_2 - r_1}{r_{av}}\right]^2\right\}^{1/2} \tag{63}$$

$$r_{av} = \frac{r_1 + r_2}{2}$$

$$\sin\bar{\phi} = \sin(\phi_{av})\sin\left[\frac{\frac{\phi_2 - \phi_1}{2}}{\frac{\phi_2 - \phi_1}{2}}\right] \tag{64}$$

and

$$\phi_{av} = \frac{d_2 + d_1}{2}$$

In TRUMP input data the following dimensional factors are specified:

$$d_r = \bar{r} \qquad \left(\cong r_{av}, \text{ if } (r_2 - r_1) < \frac{r_{av}}{6}\right) \tag{65}$$

$$d_w = r_2 - r_1 \tag{66}$$

and

$$d_\ell = \sin\frac{\bar{\phi}}{2}\left[\frac{(\phi_2 - \phi_1)(\theta_2 - \theta_1)}{2\pi}\right] \tag{67}$$

In the calculations, an equidistant mesh with $r_2 - r_1 = 0.1$ was used. Due to symmetry, only hemispheres were used, so $d_\ell = 0.5$. Finally, $d_r = \bar{r}$ is as given in Table 2.

Table 2. Values of r, r_{av}, and $\bar{r}$ for the hemisphere particles (meters).

r	r_{av}	$d_r = \bar{r}$
0		
	.05	5.7735×10^{-2}
0.1		
	0.15	1.5275×10^{-1}
0.2		
	0.25	2.5166×10^{-1}
0.3		
	0.35	3.5119×10^{-1}
0.4		
	0.45	4.5092×10^{-1}
0.5		
	0.55	5.5076×10^{-1}
0.6		
	0.65	6.5064×10^{-1}
0.7		
	0.75	7.5056×10^{-1}
0.8		
	0.85	8.5049×10^{-1}
0.9		
	0.95	9.5044×10^{-1}
1.0		
	1.05	1.0504
1.1		
	1.15	1.1504
1.2		
	1.25	1.2503
1.3		
	1.35	1.3503
1.4		
	1.45	1.4503
1.5		

A comparison of the numerical and analytical results is presented in Figure 13. In this simulation, the fracture was divided into 25 nodes increasing in size from the inlet as 15 m (10), 30 m (10) and 100 m (5). The spherical particles were divided into 15 equidistant nodes with $\Delta r = 0.1$ m. The solution in Figure 13 pertains to a point in the fracture at z = 225 m.

Problem 4: Case 2 with Radioactive Decay

We now consider the case in which the species in Problem 2 is allowed to undergo radioactive decay with a decay constant λ_d. That is, on the left-hand side of (37) and (38) we add, respectively, $-\lambda_d c_f$ and $\lambda_d K c_p$. In addition, we also modify the boundary condition (39) by, $c_f(0,t) = c_o e^{-\lambda_d t}$. This boundary condition simulates the constant leach rate of a body containing a decaying nuclide. For this case the analytical solution is simply given by:

$$\left.\frac{c_f}{c_o}\right|_{\lambda_d>0} = e^{-\lambda_d t} \left.\frac{c_f}{c_o}\right|_{\lambda_d=0} \tag{68}$$

The case with $D_L = 10^{-5}$ m^2/sec of Problem 2 was repeated with two values of λ_d: $\lambda_d = 8.6643 \times 10^{-7}$ Sec^{-1} and 8.6643×10^{-8} Sec^{1}, corresponding to half lives of about 9.259 and 92.59 days, respectively. The results of the numerical simulations are given in Figure 14 for a point at z = 0.475 m. A general good agreement is seen except for a slightly earlier break-through obtained in the numerical solution.

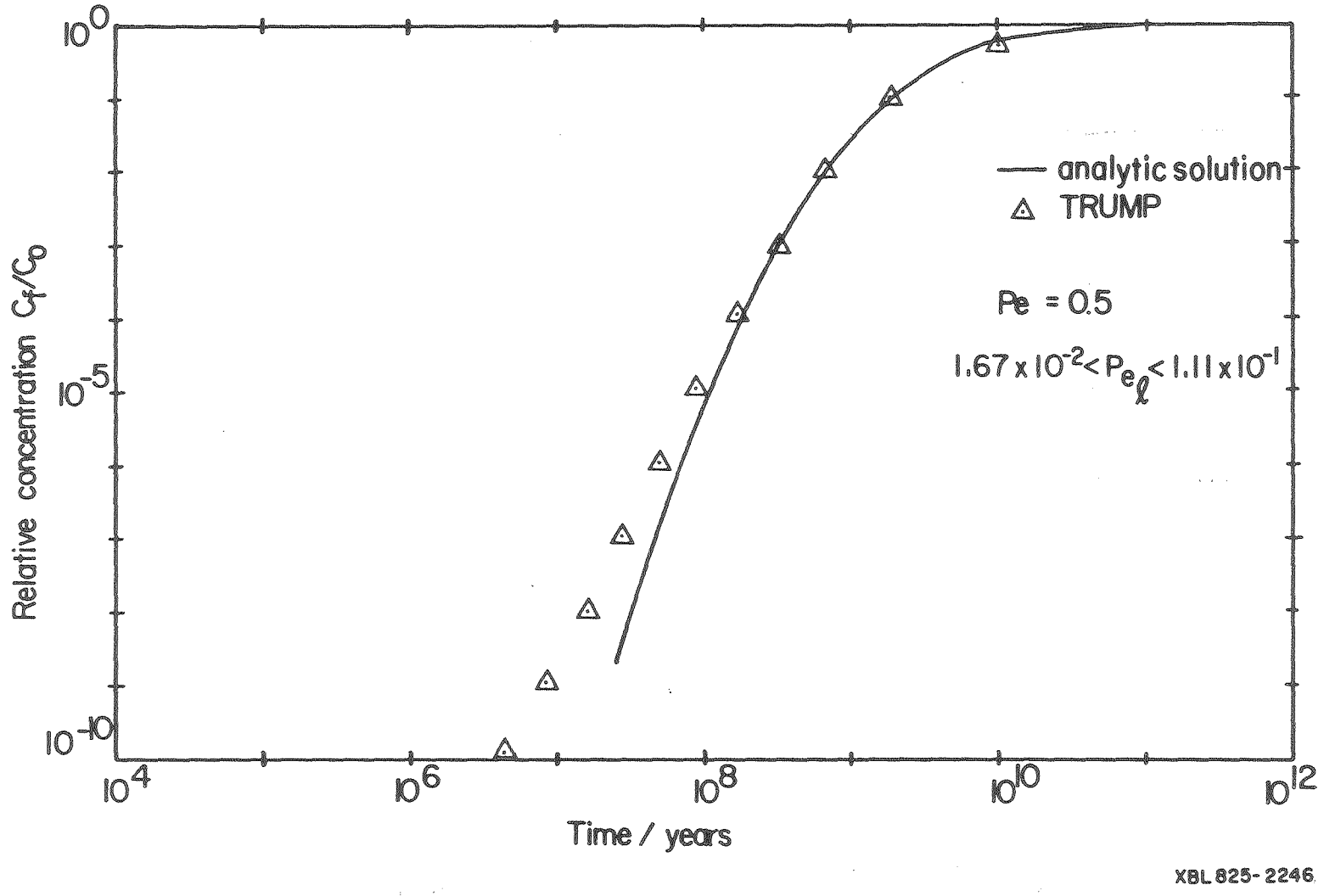

Figure 13. Penetrating case: Comparison of analytic and numerical solutions for a mesh with $0.0167 < Pe_\ell < 0.111$ and $Pe = 0.5$. [XBL 825-2246]

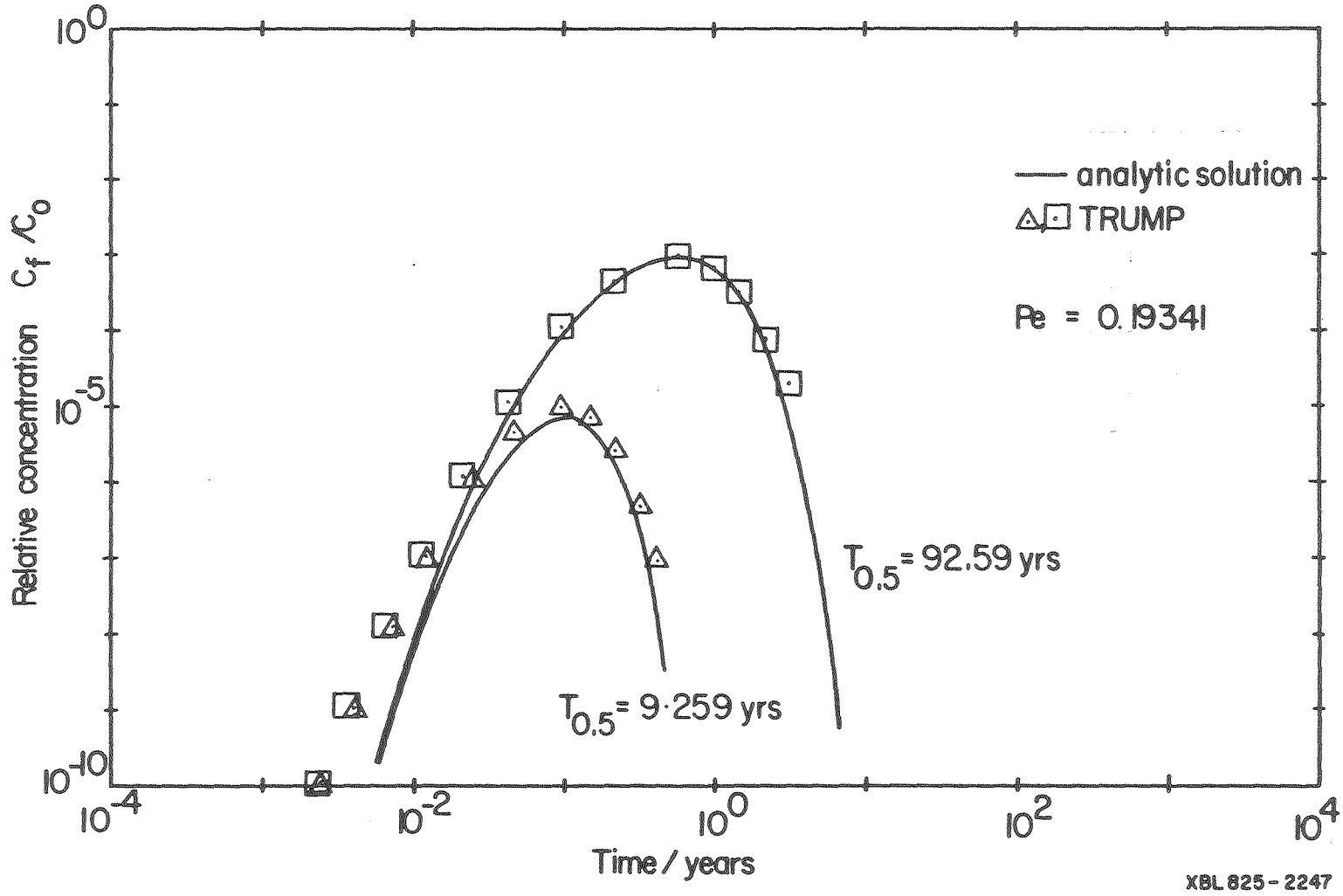

Figure 14. Nonpenetrating case with decay: Comparison of analytic and numerical solutions for a mesh with $0.005 < Pe_\ell < 0.041$ and with half-lives of 8×10^5 and 8×10^6 s. [XBL 825-2247]

Problem 5: Case 3 with Radioactive Decay

Just as in Problem 4, a decay constant of $\lambda_d = 2.3105 \times 10^{-9}$ yr^{-1} was included in Problem 3. This corresponds to a half-life of about 3×10^8 years. The results of the simulation are presented in Figure 15 for a point in the fracture at z = 225 m. Here too, good agreement is seen except for an earlier numerical break-through.

SENSITIVITY ANALYSIS

A prime motivation for the present study was a desire to evaluate the magnitude with which available numerical methods can match solutions to partial differential equations. Ideally, it is desirable to be able to attain accuracies of 10^{-4} to 10^{-5} percent since in the disposal of high-level radioactive wastes such relative concentrations might be hazardous in the biosphere. Our study shows that it is possible to attain accuracies of 10^{-3} to 10^{-4} percent under ideal conditions using numerical techniques.

Nevertheless, the very real question exists as to whether the partial differential equation itself realistically depicts nature, or whether all the coefficients in the differential equation are known with certainty. To investigate the latter question, a series of sensitivity studies were made.

A simplified sensitivity analysis was performed using the analytical solutions presented by Neretnieks (1980) and by Rasmuson and Neretnieks (1980). Neglecting longitudinal dispersion in the fractures and assuming infinite block size, the concentration in a point z downstream (Neretnieks, 1980) is:

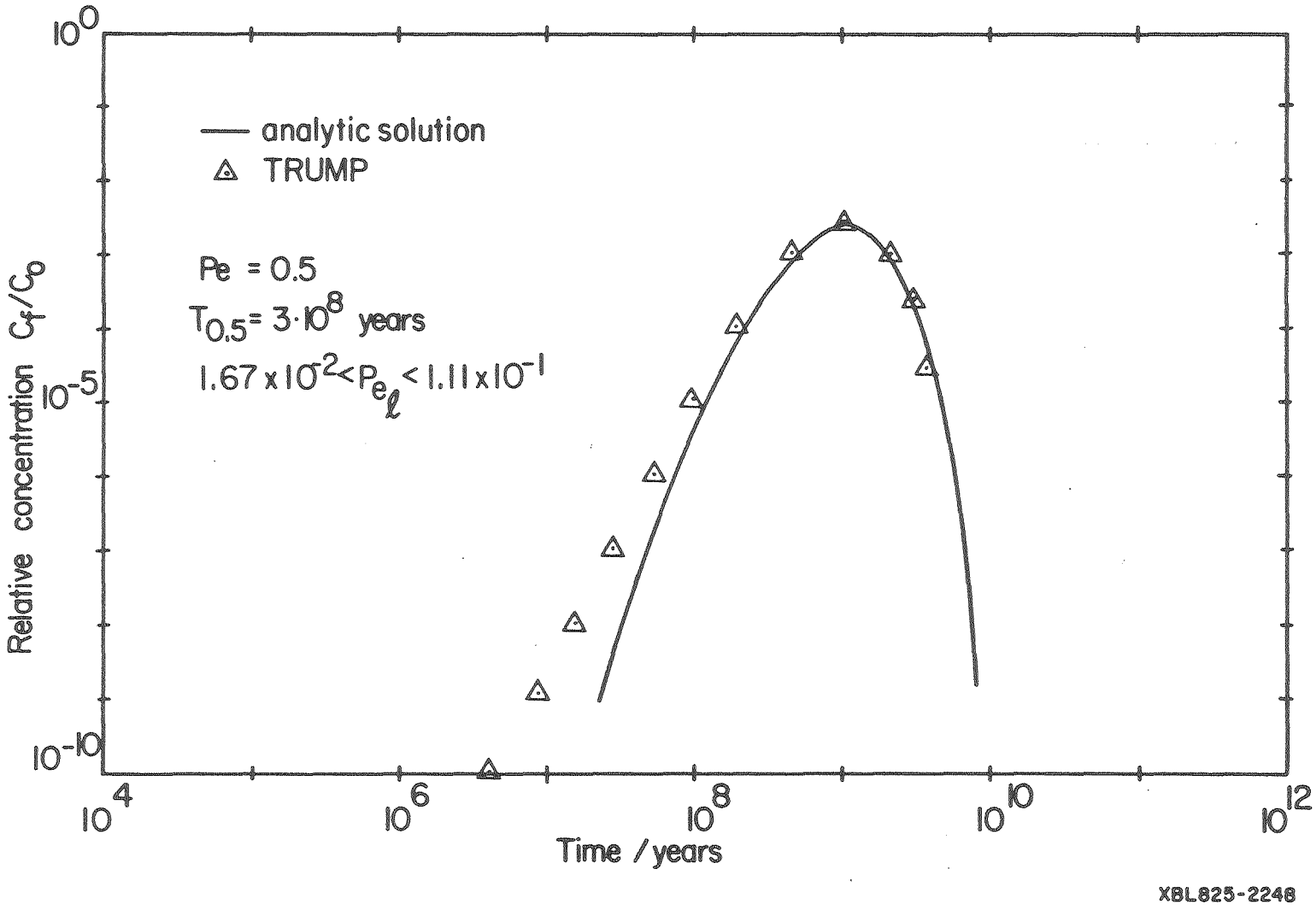

Figure 15. Penetrating case with decay: Comparison of analytic and numerical solutions for a mesh with $0.0167 < Pe_\ell < 0.111$ and with half-life of 3×10^8 years.
[XBL 825-2248]

$$\frac{c}{c_o} = c^{-\lambda_d t} \operatorname{erfc} \frac{G}{\sqrt{t - t_w}} \tag{69}$$

where

$$G = \frac{D_p \epsilon_p z}{K_p i S \sqrt{D_a}}, \qquad D_a = \frac{D_p \epsilon_p}{K}, \qquad \text{and} \qquad t_w = \frac{z}{v_f}.$$

The peak concentration can be found by differentiating equation (69). In the analysis, a central case was chosen where $(c/c_o)_{max} = 1.0 \times 10^{-5}$. By variation of the parameters the relative change in $(c/c_o)_{max}$ is found. The sensitivity S_i of the peak concentration to a perturbation of a parameter i is defined as:

$$S_i = \frac{\Delta\ (c/c_o)_{max}\ /\ (c/c_o)_{max}}{\Delta\ \text{parameter}_i\ /\ \text{parameter}_i} \tag{70}$$

Table 3 shows the parameter values which determine the base case (1). For these values $(c/c_o)_{max} = 1.0 \times 10^{-5}$.

Table 3 Specification of base cases used in sensitivity study.

Parameter	Dimension	1	2
$D_p\epsilon_p$	m^2/s	10^{-12}	10^{-12}
K	m^3/m^3	170	810
z	m	2250	300
K_p	m/s	10^{-9}	10^{-7}
i	m/m	0.01	0.01
S	m	50	50
$T_{1/2}$	years	3.10^6	13.2
Pe	-	∞	3.33

The sensitivity of $(c/c_o)_{max}$ to a variation in the Peclet number was investigated using the analytical solution in Rasmuson and Neretnieks (1980). The parameter values used as reference case are given in the last column (2) of Table 3. In this case, $(c/c_o)_{max} = 8.8 \times 10^{-6}$. The sensitivities obtained from equation (70) are given in Table 4.

Table 4 Sensitivity of $(c/c_o)_{max}$ to variation in parameters.

Parameter	S_i
$D_p\varepsilon_p$	- 4.1
K	- 4.1
z	- 6.6
K_p	+ 16
i	+ 16
S	+ 16
Pe	- 1.7

The sensitivities are very large. A 10% increase in $D_p\varepsilon_p$ or K would decrease $(c/c_o)_{max}$ from 1.0×10^{-5} to 0.6×10^{-5}, whereas a 10% increase in K_p, i or S would increase $(c/c_o)_{max}$ to 2.6×10^{-5}. As natural variations in these parameters are larger than 10%, it will probably not be possible to predict $(c/c_o)_{max}$ with an accuracy better than half an order of magnitude, for this part of the break-through curve. The sensitivity of $(c/c_o)_{max}$ to variations in the Peclet number is smaller than for the other parameters. A 10% increase in Pe would decrease $(c/c_o)_{max}$ from 8.8×10^{-6} to 7.3×10^{-6}. However, the uncertainty in the Peclet number is considered to be very large.

CONCLUSION

The ability of the conceptual model to describe flow and mass transfer in fissured rock is not proven. In view of this and the sensitivity of numerical accuracy to input data, the method used is more than adequate at present for practical applications.

ACKNOWLEDGMENT

This work was supported by the Director, Office of Energy Research, Office of Basic Energy Sciences, Division of Engineering, Mathematics, and Geosciences of the U. S. Department of Energy under Contract Number DE-AC03-76SF00098. Two of the authors, Rasmuson and Neretnieks, were funded by the Nuclear Fuel Safety project in Sweden.

REFERENCES

Carslaw, H. S. and Jaeger, J. C., Conduction of Heat in Solids, Oxford Clarendon Press, 1973.

Dillon, R. T., Lantz, R. B., Pahwa, S. B., Risk methodology for geologic disposal of radioactive waste. The Sandia Waste isolation flow and transport model, Sand 78-1267, NUREG/CR-0424; Sandia 1978.

Edwards, A. L., TRUMP: A computer Program for transient and Steady state Temperature Distributions in Multidimensional Systems, National Technical Information Service, National Bureau of Standards, Springfield, Va., 1969.

Fried, J. J. and Combarnous, M. A., Dispersion in porous media, Advances in Hydroscience, V. T. Chow, ed., 7, 170 (1971).

Grisak, G. E. and Pickens, J. F., Solute transport through fractured media, 1. The effect of matrix diffusion, Water Resour. Res.,16, 719, 1980

Grisak, G. E., Pickens, J. F., and Cherry, J. A., Solute transport through fractured media, 2. Column study of fractured till, Water Resour. Res., 16, 731, 1980

Grisak, G. E., Pickens, J. F., An analytical solution for transport through fractured media with matrix diffusion. J. Hydrol., 52, 47, 1981.

KBS (Nuclear Fuel Safety Project), Handling of spent nuclear fuel and final storage of vitrified high-level reprocessing waste, IV. Safety analysis, Stockholm, 1977.

KBS (Nuclear Fuel Safety Project), Handling and final storage of unreprocessed spent nuclear fuel, II. Technical, Stockholm, 1978.

Lester, D. H., Jansen, G., Burkholder, H. C., Migration of radionuclide chains through an adsorbing medium, AIChE Symposium series No 152 71 (1975), p 202.

Narasimhan, T. N., A perspective on numerical solution of the diffusion equation, Advances in Water Resources, 1, 147-155, 1978.

Narasimhan, T. N. and Witherspooon, P. A., An Integrated Finite Difference Method for analyzing fluid flow in porous media, Water Resources Res., 12, 57-64, 1976.

Narasimhan, T. N., Witherspoon, P. A., and Edwards, A. L., Numerical model for saturated-unsaturated flow in deformable porous media, Part 2. The Algorithm, Water Resources Res., 14, 255-261, 1978.

Narasimhan, T. N., Neuman, S. P., and Witherspoon, P. A., Finite element method for subsurface hydrology using a mixed explicit-implicit iterative scheme, Water Resour. Res., 14(5) 863-877, 1978.

Neretnieks, I., Analysis of some washing experiments of cooked chips. The Swedish Paper J. 75, 819, 1972.

Neretnieks, I., Diffusion in the rock matrix--an important factor in radionuclide retardation? J. Geophys. Res., 85, 4379, 1980.

Rasmuson A., Diffusion and sorption in particles and two-dimensional dispersion in a porous medium, Water Resour. Res., 17, 321, 1981.

Rasmuson, A. and Neretnieks, I., Exact solution of a model for diffusion in particles and longitudinal dispersion in packed beds AIChE.J., 26, 686-690, 1980.

Rasmuson, A. and Neretnieks, I., Migration of radionuclides in fissured rock--the influence of micropore diffusion and longitudinal dispersion, J. Geophys. Res., 86, 3749, 1981.

Snow, D. T., Rock fracture spacings, openings and porosities. J. Soil Mech. Found. Div., Amer. Soc. Civil. Eng., 94 (SM1), 73, 1968.

Tang, D. H., Frind, E. O., and Sudicky, E. A., Contaminant transport in fractured porous media: Analytical solution for a single fracture. Water Resour. Res., 17, 555, 1981.

Witherspoon, P. A., Wang, J. S. Y., Iwai, K., and Gale, J. E., Validation of cubic law for fluid flow in a deformable rock fracture, Earth Sciences Division, Lawrence Berkeley Laboratory, Berkeley, California 94720, LBL-9557, 1979.

NOTATION

$A_{\ell,k}$	area of the connection between nodes ℓ and k.	L^2
b	half-width of fissure	L
c	concentration	M/L^3
c_f	concentration in liquid in fissures	M/L^3
c_p	concentration in liquid in microfissures	M/L^3
c_s	concentration of solute in the solids defined as mass of solutes per unit volume of the porous medium	M/L^3
c_o	inlet concentration in the liquid	M/L^3
c_o^{ℓ}	concentration at node ℓ at t_o	M/L^3
$c_{\ell,b}$	concentration at the boundary surface segment $\Delta\Gamma_{\ell,b}$ of node ℓ	M/L^3
$\bar{c}_r$	volume averaged concentration in blocks	M/L^3
$\bar{c}_{\ell,m}$	mean concentration at the interface between volume elements ℓ and m	M/L^3
c_Γ	mean concentration at the surface Γ	M/L^3
Δc	difference in concentration	M/L^3
$\bar{C}_\ell$	capacity of volume element ℓ defined as the mass of solute released or taken into storage per unit change in concentration	$1/L^3$
d_ℓ	half-width of a rectangular plume element	L
$d_{\ell,i}$, $d_{m,i}$	distances from nodes ℓ and m to the interface between them	L
D	effective diffusivity in bulk solid; $= D_p\epsilon_p$. Also used as a general symbol for diffusivity	L^2/T

D_L	longitudinal dispersion coefficient	L^2/T
D_ℓ	effective diffusivity of node ℓ	L^2/T
D_p	diffusivity in water in pores	L^2/T
$D_{f,r}$	diffusivity at the fracture-rock interface	L^2/T
$F_{\ell,b}$	volumetric fluid flux between the boundary and node ℓ	L^3/T
$F_{\ell,m}$	volumetric fluid flux between nodes ℓ and m	L^3/T
i	hydraulic gradient	L/L
k_f	mass transfer coefficient	L/T
K	volume equilibrium constant	L^3/L^3
K_A	distribution coefficient or partition coefficient, defined by $K_A = c_s/c_p$	L^3/L^3
K_ℓ	volume equilibrium constant of element ℓ	L^3/L^3
K_p	hydraulic conductivity of the bulk rock	L/T
m	$= \varepsilon_f/(1 - \varepsilon_f)$	
$\bar{n}$	unit outer normal	
p	iteration number	
Pe	Peclet number for analytical solution defined as $Pe = v_f z/D_L$ (equation 52)	
Pe_ℓ	local Peclet number for element ℓ in the numerical solution, given by $Pe_\ell = v_f \Delta z/2D_L$ (equation 24)	
$\vec{q}$	Darcy velocity	L/T
r_o	effective spherical radius	L
r	radial distance from center of spherical particle	L
R	= K/m, distribution ratio	

R_F	$= r_o/3k_f$, film resistance	T
S	fissure spacing	L
S_i	sensitivity	
t	time	T
t_o	initial time	T
$\Delta t_{stab,\ell}$	time constant or stable time step for node ℓ	T
T'	dimensionless time; $T' = D_p \varepsilon_p t/Kr_o^2$	T
$T_{1/2}$	half-life	T
$U_{\ell,b}$	conductance at the boundary surface segment $\Delta\Gamma_{\ell,b}$ of volume element ℓ	L^3/T
$U_{\ell,m}$	conductance between nodes ℓ and m	L^3/T
v_f	average velocity of water in fissures	L/T
V_b	volume of rock, fracture system; $V_b = V_r + V_f$	L^3
V_f	volume of fracture	m^3
V_ℓ	volume of element ℓ	L^3
V_r	volume of rock matrix	L^3
w	rate of generation of solute.	M/L^3T
y	$= \sigma t$, contact time parameter	
z	distance in flow direction	L
Δz	length of a volume element in a one-dimensional problem	L
Z_ℓ	sum of the conductances and advectances over the surface Γ enclosing element ℓ	L^3/T

α	a parameter relating time constant of an element to the first arrival of solute	
β	mesh spacing factor	
γ	$= 3D_p\varepsilon_p/r_o^2$	T^{-1}
Γ	closed surface bounding an element	L^2
$d\Gamma$, $\Delta\Gamma$	an elemental segment of Γ	L^2
Γ_b	surface segment on the external boundary of flow region	L^2
Γ_i	surface segment interior to the flow region	L^2
$\Delta\Gamma_{\ell,m}$	surface segment separating nodes ℓ and m	L^2
δ	$= \gamma z/mv_f$, bed-length parameter	
ε_f	porosity of fissures	
ε_p	porosity of rock matrix	
ζ	upstream weighting factor	
θ	implicit weighting factor for the time domains	
λ	variable of integration	
λ_d	decay constant of radionuclide	T^{-1}
ν	$= \gamma R_F$	
σ	$= 2D_p\varepsilon_p/Kr_o^2$	T^{-1}